Modeling of reactive transport with particle tracking and kernel density estimators

Maryam Rahbaralam

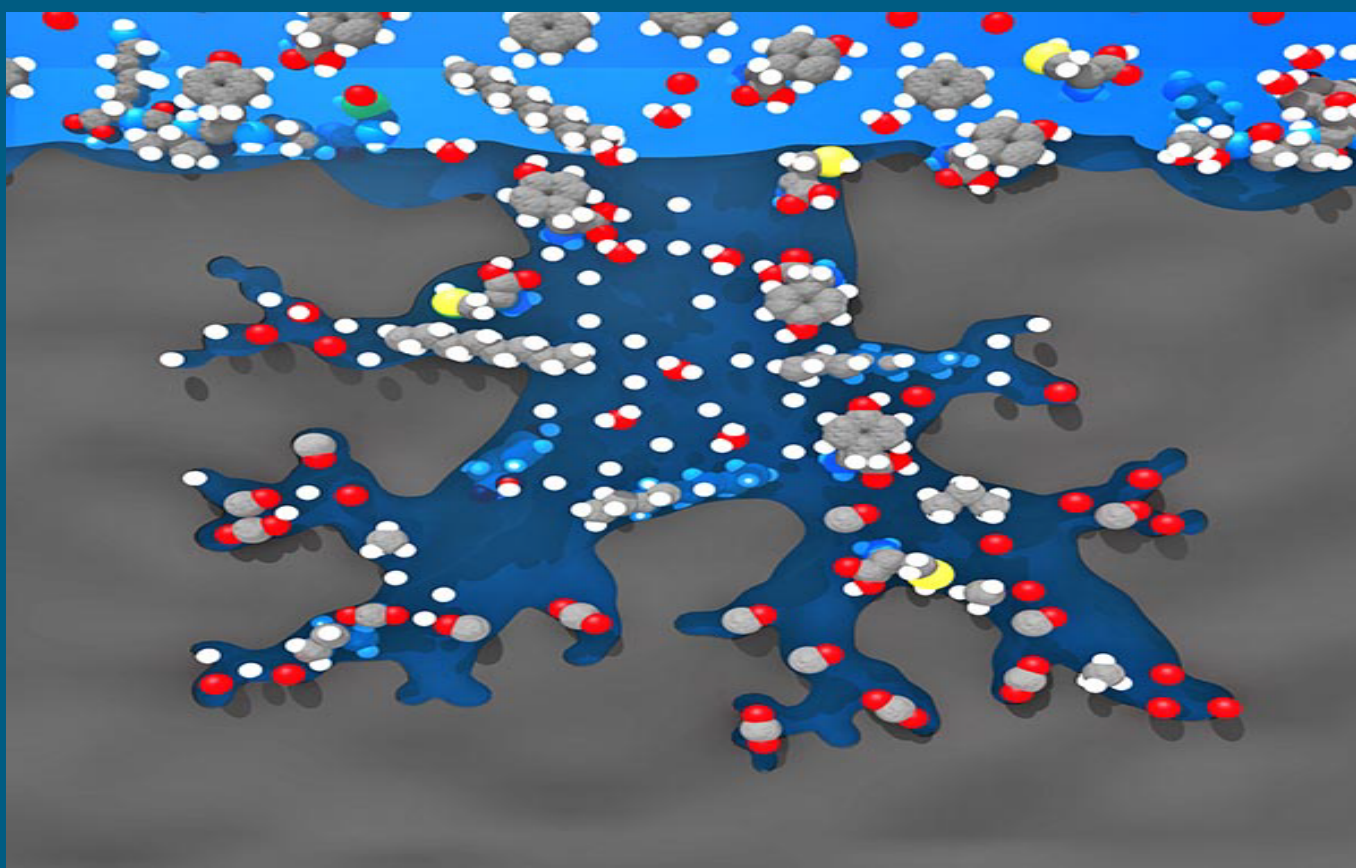

Doctoral Thesis
Barcelona, September 2017

Modeling of reactive transport with particle tracking and kernel density estimators

Maryam Rahbaralam

Doctoral Thesis
Advisors: Daniel Fernàndez-Garcia and Xavier Sánchez
Barcelona, September 2017

Departamento de Ingeniería Civil y Ambiental
Programa de Doctorat de Hidrología Subterránea (GHS)

Abstract

Modeling of reactive transport with particle tracking and kernel density estimators

Maryam Rahbaralam

Random walk particle tracking methods are a computationally efficient family of methods to solve reactive transport problems. While the number of particles in most realistic applications is in the order of $10^6 - 10^9$, the number of reactive molecules even in diluted systems might be in the order of fractions of the Avogadro number. Thus, each particle actually represents a group of potentially reactive molecules. The use of a low number of particles may result not only in loss of accuracy, but also may lead to an improper reproduction of the mixing process, limited by diffusion. Recent works have used this effect as a proxy to model incomplete mixing in porous media. The main contribution of this thesis is to propose a reactive transport model using a Kernel Density Estimation (KDE) of the concentrations that allows getting the expected results for a well-mixed solution with a limited number of particles. The idea consists of treating each particle as a sample drawn from the pool of molecules that it represents; this way, the actual location of a tracked particle is seen as a sample drawn from the density function of the location of molecules represented by that given particle, rigorously represented by a kernel density function. The probability of reaction can be obtained by combining the kernels associated with two potentially reactive particles. We demonstrate that the observed deviation in the reaction vs time curves in numerical experiments reported in the literature could be attributed to the statistical method used to reconstruct concentrations (fixed particle support) from discrete particle distributions, and not to the occurrence of true incomplete mixing. We further explore the evolution of the kernel size with time, linking it to the diffusion process. Our results show that KDEs are powerful tools to improve computational efficiency and robustness in reactive transport simulations, and indicates that incomplete mixing in diluted systems should be modeled based on alternative mechanistic models and not on a limited number of particles.

Motivated by this potential, we extend the KDE model to simulate nonlinear adsorption which is a relevant process in many fields, such as product manufacturing or pollution remediation in porous materials. We show that the proposed model is able to reproduce the

results of the Langmuir and Freundlich isotherms and to combine the features of these two classical adsorption models. In the Langmuir model, it is enough to add a finite number of sorption sites of homogeneous sorption properties, and to set the process as the combination of the forward and the backward reactions, each one of them with a pre-specified reaction rate. To model the Freundlich isotherm instead, typical of low to intermediate range of solute concentrations, there is a need to assign a different equilibrium constant to each specific sorption site, provided they are all drawn from a truncated power-law distribution. Both nonlinear models can be combined in a single framework to obtain a typical observed behavior for a wide range of concentration values. This approach opens up a new way to predict and control an adsorption-based process using a particle-based method with a finite number of particles.

Finally, by classifying the particles to mobile and immobile states and employing transition probabilities between these two states, we take into account the porosity of the diluted system in the KDE model. The state of a particle is an attribute that defines the domain at which the particle is present at a given time within the porous medium. The transition probabilities are controlled by two parameters which implicitly determine the porosity. Simulations results show a good agreement with the analytical solutions of complete and incomplete mixing solutions, independent of the number of particles. A transition between the complete and incomplete mixing solutions is also obtained, showing a good match with a transition probability function. These results show the potential of our proposed model to simulate reactive transport problems in porous media.

Acknowledgments

First and foremost I offer my sincerest gratitude to my supervisors, Professor Daniel Fernàndez-Garcia and Professor Xavier Sánchez, who have supported me throughout my research and thesis with their patience and knowledge whilst allowing me the room to work in my own way. It has been an honor and a privilege to work with them and I am deeply grateful for the opportunity to have done so. I am also truly indebted and thankful to my husband Professor Amir Abdollahi for his guidance and support.

I would like to appreciate the faculty of Civil and Environmental Engineering Department, in particular Professor Alonso Pèrez de Agreda, who gives me this opportunity to be a member of Hydrogeology Group (GHS). My gratitude also goes to Professors Jesús Carrera, Carlos Ayora, Maarten Saaltink and Enric Vázquez for their support. I would also like to thank the reviewers of the thesis and the members of the committee for their useful comments and advice. I humbly acknowledge the assistance of administrative staff Teresa, Silvia and the technical support of Albert.

It has been a privilege to share so many moments with my officemates and fellow postgraduate students in the group of Hydrogeology. Among them I want to mention especially Carme Barba, Nuria, Albert Carles, Albert Folch , Paula, Francesca, Laura, Michela, Sonia, Lurdes and Meritxell. I am very grateful for their true friendship and support through the years.

I owe sincere and earnest thankfulness to my family, especially my husband, for their unconditional love, patience, support and encouragement through all my life. Their love has provided me with the enthusiasm to face new projects and constantly seek novel challenges.

I gratefully acknowledge the financial support from the AGAUR (Generalitat de Catalunya) through the grant for universities and research centres for the recruitment of new research personnel (FI-DGR 2013, FI-DGR 2014).

Finally, my thanks also go to those who, directly or indirectly, helped me to finish my thesis.

Contents

List of Figures

List of Tables

Thesis body

1 Introduction

The complexity associated with the simulation of the interactions between flow, transport, and chemical processes requires developing reliable, as well as predictive, reactive transport models. A major challenge in this area is the incorporation of the interaction of the reactants facilitated by pure diffusion into a dynamic system. This problem has traditionally been addressed in porous media using a diffusion-reaction equation. The main interest has typically relied on finding or fitting the proper parameters that describe the experimental or field observations. This generic problem, posed in terms of the spatial and temporal distribution of reactants and products, has practical applications especially in the groundwater remediation context, where the choice of remediation strategy is based on accurate modeling of the anticipated degradation rate of the contaminants. Other applications include drug delivery in biological systems (Saurabh and Chakraborty, 2009), geological CO2 sequestration (Xu et al., 2011), chemical weathering (Li et al., 2014), and enhanced oil recovery (Gogoi, 2011), to name a few.

In most natural systems, the rate of reactions between the chemical species is limited by mixing because the molecules can only react when they come into physical contact to allow the corresponding bonds to occur. In well-mixed systems, like a stirred laboratory beaker, the spatial fluctuations in concentrations of the chemical species are negligible, and the rate of reaction is spatially uniform. However, if the mixing process is slow in comparison with the reaction rate, a mixing-limited regime will appear. In this regime, and when the initial spatial distribution of reactants is heterogeneous, the magnitude of concentrations as a function of time fluctuate significantly and segregated areas (islands) of one reacting species start to form in the domain (Bolster et al., 2012; Tartakovsky and Meakin, 2005). This segregation of the species is dictated by the reduced area of contact between reactants and was described from theoretical and numerical viewpoints several decades ago (Ovchinnikov and Zeldovich, 1978; Kang and Redner, 1985). Thus, it comes as no surprise that the prediction of reactions based on the well-mixed assumption associated with the classical transport and reaction equations within systems ranging from homogeneous systems (Gramling et al., 2002; Raje and Kapoor, 2000) to heterogeneous systems (Willmann et al., 2010) are bound to failure.

The study of solute transport driven by diffusion is one of the classical problems where

the dichotomy between Eulerian and Lagrangian approaches has been traditionally well explained. An Eulerian approach implies setting the problem in terms of concentration of reactant species, and then postulating some macroscopic laws (either empirical or deduced from thermodynamic considerations) to describe the reaction rate based on such concentrations. The problem is then formulated from macroscopic mass balance equations such as, for example, the advection-dispersion-reaction equation (ADRE). Concentration is a macroscopic quantity (mass per unit volume) and thus it has no meaning when the volume reduces to zero. An alternative is to study the process at the molecular level, theoretically tracking the movement and fate of each individual molecule, within a Lagrangian framework (Gillespie, 2000, 1977, 1976). This alternative is obviously unfeasible, as even minute concentrations result in a extremely large number of molecules (1 mol equals 6.02×10^{23} molecules); furthermore, equations of the continuum are no more applicable, and reactions should be assessed from collision theory.

Particle Tracking Methods (PTM) try to combine both approaches to provide an efficient solution to reactive transport simulations. The idea is to split the total mass into a number of particles (typical orders are $10^6 - 10^9$), many orders of magnitude lower than the actual number of molecules, and devise a way to reconstruct the spatial and temporal distribution of concentrations of the different species from the location of particles at any given time. This methodology has obvious drawbacks such as: (1) the estimation of macroscopic quantities (concentrations) from discrete particle information being a non-unique process, and (2) the need to set up reactive rules applied to a finite number of particles so that, when upscaled, they properly represent reaction rules observed at the macroscale. An additional drawback would be the modeler's choice of the number of particles, and more, the meaning of the concept particle itself.

Regarding the first problem, recently an optimal method for the reconstruction of concentrations and their functionals based on Kernel Density Estimators (KDE) was developed (Fernàndez-Garcia and Sanchez-Vila, 2011). This method has been successfully applied to estimate concentrations of conservative and reactive species (Henri and Fernàndez-Garcia, 2014), heavily-tailed breakthrough curves (Pedretti and Fernàndez-Garcia, 2013), reaction rates in precipitation/dissolution problems (Fernàndez-Garcia and Sanchez-Vila, 2011), and risk predictions from particle distributions (Siirila-Woodburn et al., 2015). Regarding the second point, the translation of macroscopic rules to PTM, a technique was proposed by

Benson and Meerschaert (Benson and Meerschaert, 2008) to study reactive transport for a bimolecular reaction, introducing an algorithm that accounts for the probability that two individual particles react as a function of their relative distance; this method was an extension of the original algorithm proposed by Gillespie (Gillespie, 2000) to simulate batch reactions in a stochastic framework at the molecular level. The method avoids the need to continuously reconstruct concentration maps during the course of the simulation for each individual time step, considered the main disadvantage of PTM (Salamon et al., 2006b; Boso et al., 2013).

Here we combine these two ideas to develop a KDE model that can be directly used to study bimolecular reaction in diffusive problems. The main idea is to use Kernels to provide a new weighting functions for particles to interact following Benson and Meerschaert (Benson and Meerschaert, 2008) approach. In this case, when particles are transformed into another species or mineral, the shape of the Kernel automatically adjust, expanding its region of influence and the region of interaction between particles (Fernàndez-Garcia and Sanchez-Vila, 2011). This method increases the number of particles that could react at a given time. The introduction of this expanding Kernel provides some insights into a problem that has been recently raised in the literature. Benson and coworkers have studied the evolution of concentration with time in a bimolecular reactive problem susceptible to incomplete mixing (Benson and Meerschaert, 2008; Bolster et al., 2012; Benson and Meerschaert, 2009). These authors represented incomplete mixing by setting up a low number of particles into the reactive system; the lower the number of particles the earlier reaction became limited. This was shown later on to represent a continuum-scale model based on the ADRE with stochastic noisy initial conditions (Ding et al., 2013; Paster et al., 2014). While this is an intelligent approach, we would like to stress that caution should be taken when using the statistical fluctuations of a histogram, produced by sub-sampling the concentrations, to represent a true physical phenomenon. The analogy is only valid when the number of molecules is really limited or in systems with noisy initial concentrations. Other physical processes leading to incomplete mixing such as rate-limited mass transfer at the pore-scale (Sanchez-Vila et al., 2010) or heterogeneity in the hydraulic properties at a larger scale (Castro-Alcala et al., 2012) might not be properly represented.

We thus associate incomplete mixing in some applications to the combination of low number of particles combined with an estimation of concentrations based on the particles

having a zero support size .e.g., (Pollock, 1988; Salamon et al., 2006b). We contend that the limited number of particles should not be considered as a tool for generating incomplete mixing systems. To make this point we show how our approach based on the inclusion of optimal KDEs allows reproducing complete mixing up to a very small number of particles. We contend then that incomplete mixing in diluted systems should be modeled based on alternative mechanistic models, see (Sanchez-Vila et al., 2010), and not on a limited number of particles.

Motivated by this potential, we extend the KDE model to simulate adsorption which is defined as the binding of atoms or molecules from a gas or liquid to a surface. It is a phenomenon well-described in many physical, biological, and chemical systems and processes, and that has been widely employed in industrial applications such as pharmaceutical industry, chillers and air conditioning systems, water purification, coatings, and resins, to name a few. To design and optimize an adsorption-based process, it is necessary to characterize accurately the adsorption equilibria and their dependence on the experimental conditions. Equilibrium relations are described by adsorption isotherms, relating the equilibrium concentration of a solute on the surface of an adsorbent to the concentration of the solute in the liquid/gas being in contact. In 1916, Langmuir introduced the first scientifically based nonlinear isotherm by assuming a homogeneous surface with a specific number of sites where the solute molecules could be adsorbed (Langmuir, 1918). This author assumed that the adsorption involves the attachment of only one layer of molecules to the surface, i.e. mono-layer adsorption. However, the Langmuir model deviates from the experimental observations in the presence of a rough inhomogeneous surface where multiple site-types or layers are available for adsorption and some parameters vary from site to site. This problem was tackled by Freundlich who proposed the first mathematical fit to a nonlinear isotherm, leading to a purely empirical formula for adsorption on heterogeneous surfaces (Freundlich, 1906). The Freundlich isotherm was established by assuming that adsorption varies directly with pressure without reaching saturation, while experimentally the rate of adsorption saturates by applying very high pressures. Therefore, the use of the Freundlich isotherm is appropriate when dealing with low/medium pressures/concentrations. We show that the adsorption model proposed is able to reproduce the results of the Langmuir and Freundlich isotherms and to combine the features of these two classical models. This approach opens up a new way to predict and control an adsorption-based process using a particle-based

method with a finite number of particles.

Finally, by classifying the particles to mobile and immobile states and employing transition probabilities between these two states, we take into account the existence of a double porosity in a porous medium. To do this, the state of a particle is considered as an attribute that defines the domain at which the particle is present at a given time within the porous medium. The transition probabilities are controlled by two parameters: field capacity, which is the ratio of the immobile porosity to the mobile porosity, and the mass transfer coefficient controlling the mass exchange rate between the mobile and the immobile porosity. Simulations results show a good agreement with the analytical solutions of complete and incomplete mixing solutions, independent of the number of particles. A transition between the complete and incomplete mixing solutions is also obtained, showing a good match with a modified transition probability. These results show the potential of our proposed mobile-immobile model to simulate reactive transport problems in porous media. These results also demonstrate that a double or multiple porosity system can simulate a mixing-limited transport behavior as observed in laboratory and field experiments.

The structure of this thesis is as follows. The background information regarding PTM, KDEs, reactive transport and adsorption is presented in Section 2. Section 3 expands the proposed chemical reaction model using KDEs. This section also presents simulation results, verifying the reactive model. Section 4 introduces the proposed adsorption model using PTM and KDEs together with the model verification. Section 5 presents the extended mobile-immobile KDE model, taking into account the medium porosity. In each of these sections the most significant contributions are also highlighted. The last section is the conclusion of the thesis.

2 Background

2.1 Particle tracking methods

Particle tracking methods (PTM) simulate transport by injecting a large number of particles into the system. Each particle carries a given fraction of the total mass moving in dissolved state with groundwater and reacting according to some fundamental mechanisms. A large variety of mechanisms can efficiently simulate different transport phenomena. These mechanisms range from pure advection and random walk motions to complex reaction and mass transfer processes (Tompson and Dougherty, 1992; Salamon et al., 2006a; Moroni et al., 2007; Benson and Meerschaert, 2009). In a bimolecular reactive problem, it is worth noticing that the particle state is binary (e.g., it has either reacted or not), while in reality only a fraction of the pool of molecules may have reacted. We find here again a duality in the concept of representation: even though only a portion of molecules associated with one particle react, PTM adopt the result obtained from a Bernoulli trial sampled from the probability distribution of reacted molecules. In most approaches the total mass of each reactant is evenly distributed among the particles, so that the mass carried by each particle is simply given by the total mass in the system divided by the number of particles; e.g., for reactant A

$$m_{p,A} = \frac{1}{N_0} \int_{\Omega} [A_0(x)] d\Omega, \tag{1}$$

where N_0 is the number of particles selected by the modeler, $[A_0(x)]$ is the (spatially variable) concentration within a given volume Ω. In the case of uniform initial concentration equation (1) results in $m_{p,A} = [A_0]\Omega/N_0$. In this latter case, the initial position of each individual particle can be drawn from a multidimensional uniform distribution. For this reason, if the number of particles is small, the density of particles initially present in different locations can be slightly different, creating artificial initial fluctuations. Such difference would be reduced by increasing the number of particles.

Particle displacements

In a physical system, diffusion and reaction are simultaneous processes; reaction cannot take place without diffusion. In the numerical model these two contributions are modeled

by operator splitting, i.e., two subsequent processes within each simulation time step. First, the particles move by Brownian motion, and then they can react with each other. Without loss of generality, we consider the diffusion-reaction equation in 1-D. The initial locations of the A and B particles are respectively denoted by X_j^A and X_j^B, j indicating the particle number. We consider a domain interval defined as Ω. The initial particle location was drawn from a statistical uniform distribution. The diffusion of a species is modeled by a Brownian random walk motion with zero mean and variance $2D\Delta t$, being Δt the time interval. For each simulation time step, PTM describe the change of the particle species taking place between t and $t+\Delta t$. The random walk is an implementation of a Langevin equation without the drift term. Thus, the location of the particle j at a given time is a Markovian process characterized by a Brownian motion term, given by

$$X_j^i(t+\Delta t) = X_j^i(t) + \xi_t \sqrt{2D\Delta t},\ i = A, B \tag{2}$$

where ξ_t is a random number drawn at each time step from an independent (uncorrelated in space and time), normally distributed random variable with zero mean and unit variance. It has been shown that equation (2) satisfies the non-reactive diffusion equation in the limit for an infinite number of particles with infinitesimal mass (Tompson and Dougherty, 1992; Salamon et al., 2006a). The inclusion of the reaction term simply modifies the species state associated with that particle.

Reactive transport in porous media is typically described by the reactive-advective-dispersive equation. In this case, the displacement of a particle includes a drift term to account for advection. Thus, Eq. (2) extends to:

$$X_j^i(t+\Delta t) = X_j^i(t) + \xi_t \sqrt{2D_h\Delta t} + v\Delta t,\ i = A, B \tag{3}$$

where v is the flow velocity, and D_h is the hydrodynamic dispersion, assumed constant in this thesis.

2.2 Kernel Density Estimators

PTM are a convenient alternative to study molecular diffusion problems. In such cases particles can be associated to molecules. This would mean that a mole of solute should be discretized into N_A (Avogrado's number, $N_A = 6.02 \times 10^{23}$) molecules. In all practical

applications found in the literature the number of particles used to discretize a given mass is in the order of 10^6 to 10^9, e.g. (Riva et al., 2008). The traditional approach is based on considering that each particle actually represents a group of molecules. In all cases, the outcome of PTMs is typically expressed as a distribution of particle travel times at control locations and/or positions observed at different times. Since this information is discrete in nature a reconstruction process is fixed to finally convert particles into concentrations. This reconstruction process is normally seen as the main disadvantage of PTMs (Fernàndez-Garcia and Sanchez-Vila, 2011; Boso et al., 2013). This is based on the relationship between particle distributions and concentrations, which determines that concentrations are proportional to particle probability densities (PDFs). In this case particles have a representative size. This concept has been included into a family of methods named smoothed-particle hydrodynamics (SPH) (Tartakovsky and Meakin, 2005; Herrera et al., 2010), where a spatial distance (known as the "smoothing length") is defined, over which the properties of the particles are smoothed by a kernel function. This means that any physical quantity of any particle can be obtained by summing the relevant properties of all the particles which lie within the range of the kernel. Similarly to SPH methods, the approach actually taken by most of the existing particle tracking codes (Pollock, 1988; Salamon et al., 2006b) considers that particles have a zero support. All these methods share in common that they provide noisy estimates of the spatial or temporal distribution of concentrations. This is particularly disturbing when the objective is estimating concentrations, which is the case in most applications regarding stochastic hydrology or reactive transport.

Kernel Density Estimators (KDE) are powerful methods to reconstruct smooth concentrations and their functionals from discrete particle information in space and/or time (Fernàndez-Garcia and Sanchez-Vila, 2011; Pedretti and Fernàndez-Garcia, 2013). KDE methods were introduced in the late 50's (Rosenblatt, 1956) in order to improve the density estimation of the probability density function. The need of KDE methods appears crucial when estimating smoothed PDFs with frequency histograms, which are determined by counting the number of particles within a given time interval $B_j = [t_0 + (j-1)h, t + jh]$, where h is the time interval (bin size) and t_0 is the origin of the histogram. The frequency at the jth bin is determined by

$$\hat{p}_j = \sum_{i=1}^{N} \frac{1}{h} I(t_i \in B_j), \tag{4}$$

where N is the number of particles (arriving at the well location), $\hat{p}_j$ is the estimated density, t_i is the particle travel time data (t_1, ... ,t_N), and $I(.)$ is an indicator function defined as $I = 1$ if t_i is inside the bin and $I = 0$ otherwise. By definition, these estimators depend on the domain discretization, i.e., the choice of the support size and the number of particles falling into the support.

The use of a histogram provides a discontinuous box function that prevents the estimation of smooth probability density functions. Moreover, the histogram depends on its origin t_0 and the selection of the bin size h, which are arbitrary. KDE methods overcome these problems by replacing the fixed box model in the histogram by a moving weighting function as

$$\hat{p}(t) = \sum_{i=1}^{N} \frac{1}{h} K\left(\frac{t - t_i}{h}\right), \tag{5}$$

where K is a moving weighting function centered at the particle location chosen from functions of unitary area, i.e.,

$$\int K(\tau) d\tau = 1. \tag{6}$$

Although the traditional box model introduces discontinuities at the box edges, kernel estimators produces smooth functions of space and/or time. These kernel functions are weighting functions of the particle mass that defines its region of influence. By extending this approach, the concentration $c(x,t)$ of a given species at a given time t and location x can be reconstructed from the location of the particles present in the system as (Fernàndez-Garcia and Sanchez-Vila, 2011)

$$c(x,t) = \sum_{p=1}^{N(t)} \frac{m_p}{h(t)} K\left(\frac{x - X_p(t)}{h(t)}\right), \tag{7}$$

where h is the bandwidth, $N(t)$ is the number of particles at time t, m_p is the particle mass, and X_p is the particle location. By defining a region of influence for each particle, kernel estimator (7) produces smooth functions of space. The kernel shape depends on the choice of the bandwidth or support size h and the type of kernels. A variety of kernel functions can be used, among them, Gaussian kernels are usually preferred for mathematical advantages (Pedretti and Fernàndez-Garcia, 2013).

The optimal area of influence

As stated before, Kernels can be seen as a way to introduce into the solution the effect of using a subset of particles to represent a very large number of molecules. The larger the degree of undersampling, the more information should be conveyed into the kernel estimator. The degree of smoothing or the area of influence around a particle is controlled by the parameter h. If the number of particles is very large, there is no real need for kernels, and h should be very small. On the contrary, h should increase when the number of particles is not sufficient to account for a proper estimation of the spatial distribution of the concentrations. In general, a small support size combined with a finite number of particles leads to noisy estimates and the fluctuation of concentrations. Contrarily, an increase in the support size tends to oversmooth the estimated concentration distribution. Thus, an optimum choice of the support size, h^{opt}, exists. Choosing it should be based on an objective criterion about the reconstruction effort, minimizing the variance error while controlling the biasedness in the estimation. Park and Marron (1990) found the optimum bandwidth as

$$h^{opt} = R \;\; N^{-1/5}, \tag{8}$$

where R is given as

$$R = \left(\frac{\|\mathbf{K}\|_2^2}{\|\mathbf{p}''(\mathbf{x})\|_2^2 \; (\mu_2(K))^2}\right)^{1/5}, \tag{9}$$

where $\mu_2(K)$ is the second moment of K, $p''(x)$ is the second derivative of the concentration normalized by the total mass in the system, and the symbol $\|.\|_2^2$ is the L_2-norm operator, i.e. $\|\mathbf{p}(\mathbf{x})\|^2 = \int p(x)^2 dt$. It is clear that the optimal bandwidth h^{opt} in (8) grows inversely proportional to the number of particles; the smaller the number of particles, the larger the bandwidth size. This feature is particularly beneficial for developing a chemical reaction model, as mentioned later in the thesis. The second derivative of the density function $p''(x)$ needs to be also estimated. Several methods can be used for this purpose: (1) rule-of-thumb methods, (2) cross-validation methods, and (3) plug-in methods (see recent reviews of these methods by Jones et al. (1996) and Park and Marron (1990). Following a recent work by Fernàndez-Garcia and Sanchez-Vila (2011), we hereby employ the plug-in method to estimate the optimal bandwidth h^{opt}.

2.3 Adsorption

The Langmuir isotherm

The Langmuir isotherm explains adsorption by assuming that the adsorbent is an ideal solid surface composed of series of identical sites capable of binding the adsorbate. This binding is treated as a chemical reaction between the adsorbate molecule A and an empty site, B. This reaction yields an adsorbed complex C. This process can be reversed through desorption whereby the adsorbed molecule is released from the surface and the complex C is transformed to A and B. This dynamic equilibrium existing between the adsorbate and the adsorbent can be expressed as

$$A + B \rightleftarrows C. \tag{10}$$

This model assumes adsorption and desorption as being elementary processes, where the rate of forward adsorption r_f and the rate of backward desorption r_b are given by:

$$r_f = k_f[A][B], \tag{11}$$

$$r_b = k_b[C], \tag{12}$$

where k_f is the forward adsorption reaction constant, k_b is the backward desorption reaction constant, and $[X]$ denotes the concentration of species X (A, B, or C). At equilibrium, the rate of adsorption equals the rate of desorption, i.e. $r_f = r_b$, then by rearranging the terms we obtain

$$\frac{[C]}{[A][B]} = \frac{k_f}{k_b} = K_{eq}, \tag{13}$$

where K_{eq} is the equilibrium constant. By adding up the concentration of free sites $[B]$ and of occupied sites $[C]$, the concentration of all sites $[B_0]$, assumed constant in time, is obtained as $[B_0] = [B] + [C]$. Combining this relation and Eq. (13) yields the Langmuir adsorption isotherm:

$$[C] = [B_0]\frac{K_{eq}[A]}{1 + K_{eq}[A]}. \tag{14}$$

In the presence of a high concentration of $[A]$, Eq. (14) leads to the saturation of surface sites, $[C] \longrightarrow [B_0]$. In other words, the surface reaches a saturation point where the maximum adsorption capacity of the surface will be achieved.

The Freundlich isotherm

The Freundlich isotherm is an empirical model, which is commonly used to describe the adsorption performance of heterogeneous surfaces. This isotherm is mathematically expressed as

$$[C] = K[A]^m, \tag{15}$$

where K and m are called the Freundlich constants. The constant K is an adsorption coefficient, while m is a measure of the deviation from the linearity of the adsorption. Unlike in the Langmuir model, in this one there is no adsorption maximum or saturation. Equation (15) can be linearized as

$$\log[C] = \log K + m \log[A], \tag{16}$$

where m represents the slope of the line in a $log[C] - log[A]$ plot.

While the Freundlich model has been found to fit most existing adsorption experimental data (Frankenburg, 1944; Davis, 1946; Thomas, 1957; Urano et al., 1981), its theoretical basis is under scrutiny. In principle, the Freundlich isotherm can be derived from the fundamental integral equation for the overall adsorption isotherm stated as

$$\Theta_T = \int_\Omega N(Q)\Theta(Q)dQ, \tag{17}$$

where Θ_T is the relative monolayer coverage of the entire surface, N is the number of sites having adsorption energy Q, and Θ is the local coverage of individual sites. The relative coverage of the entire surface relates to the concentrations of the chemical compounds by $\Theta_T = [C]/[B_0] = [C]/([B] + [C])$. The integration region Ω is over all possible adsorption energies. It has been shown that Eq. (17) leads to the Freundlich isotherm when an exponential distribution of adsorption energies is assumed (Sips, 1948; Sheindorf et al., 1981):

$$N(Q) = m \exp(-mQ/RT), \tag{18}$$

where m and R are constants, and T is the temperature (assumed constant as implied by the word isotherm). Furthermore, it is assumed that the local coverage follows the Langmuir isotherm as

$$\Theta = \frac{\hat{K}[A]}{1 + \hat{K}[A]}. \tag{19}$$

with the equilibrium constant $\hat{K}$ depending on the adsorption energy as

$$\hat{K} = K_{eq} \exp(Q/RT). \tag{20}$$

Plugging Eqs. (18) - (20) into Eq. (17) and assuming that $Q \in (-\infty, +\infty)$ yields

$$\Theta_T = \int_{-\infty}^{+\infty} m \exp(-mQ/RT) \frac{K_{eq} \exp(Q/RT)[A]}{1 + K_{eq} \exp(Q/RT)[A]} dQ, \tag{21}$$

This integral has a solution in the form of the Freundlich isotherm given by

$$\Theta_T = \overline{K}[A]^m, \tag{22}$$

with the Freundlich constant $\overline{K} = m\pi RT {K_{eq}}^m / \sin((1-m)\pi)$. Therefore, Eqs. (17)-(22) establish a theoretical basis for the Freundlich isotherm. In Section 4, we demonstrate that this approach, which is based on an exponential distribution of adsorption energy, is mathematically equivalent to consider $\hat{K}$, in the Langmuir model, as a random variable that follows a truncated power-law distribution.

3 Chemical reaction model

This section presents our proposed chemical reaction model using KDEs. This model addresses a simple chemical reaction, i.e., a single forward bimolecular irreversible reaction $A + B \rightarrow \emptyset$. Here, two species present in the dissolved phase, A and B, react kinetically and irreversibly with unitary stoichiometric coefficients. The product of the reaction is assumed to play no role in the system (i.e., it does not produce any change in porosity or permeability). The transport of the reactants is driven by a diffusion-reaction equation with the following expression:

$$\frac{\partial C_i}{\partial t} = D\nabla^2 C_i - k_f C_A C_B, \tag{23}$$

where i stands for A, B, the concentration of species i is given by $C_i = C_i(x,t)$ (in $[ML^{-3}]$), $D[L^2T^{-1}]$ is the diffusion coefficient, and $k_f[L^3M^{-1}T^{-1}]$ is the reaction rate constant.

3.1 Analytical model

From Eq. (23), we can write that the equation satisfied by $C_A - C_B$ is conservative (i.e., not affected by geochemical reactions). If we further impose a well-mixed system, we can write

$$\frac{d}{dt}(C_A - C_B) = 0, \tag{24}$$

so that $C_A - C_B = [A_0] - [B_0]$, $[A_0]$ and $[B_0]$ being the corresponding initial concentrations. We can then use this result to rewrite the governing equation for the well-mixed concentration as

$$\frac{\partial C_A}{\partial t} = -k_f \; C_A \; (C_A + [B_0] - [A_0]). \tag{25}$$

By integrating this ODE, it is possible to write an explicit solution for the concentrations of the two species

$$C_A(t) = \frac{[A_0] - [B_0]}{1 - \frac{[B_0]}{[A_0]} exp(-k_f([A_0] - [B_0])(t - t_0))}, \tag{26}$$

and in the particular case that $[A_0] = [B_0]$, the solution is the same for both species, given by

$$C_i(t) = \frac{[A_0]}{1 + [A_0]\ k_f\ t};\ i = A, B, \tag{27}$$

indicating that $C_i(t)$ scales as $k_f^{-1}t^{-1}$ for large times.

3.2 Diffusion-based (DB) reaction

A Reactive Particle Tracking (RPT) method was recently proposed by Benson and Meerschaert (2008) (we refer to this method as the DB model). In this method, diffusion is treated by Eq. (2), and the reaction of particles is simulated through probabilistic rules,

$$P_{DB} = k_f\ m_p\ \Delta t\ v(r, \Delta t), \tag{28}$$

where P_{DB} is the probability that two particles, A and B, separated by a distance r react within a time interval Δt. It has been shown that, in the limit for an infinitely small time interval, i.e. $\Delta t \to 0$, a combination of equations (2) and (28) converges to the diffusion-reaction equation (23) (Paster et al., 2013).

Here, $v(r, \Delta t)$ is the co-location probability density function (PDF), defined as the probability that two particles initially separated by a distance r, one from species A and another from species B occupy the same position after a time interval Δt. This co-location PDF is the convolution of two Gaussian densities f_A and f_B, see Fig. 1. Assuming D constant, both PDFs have the same standard deviation $\sigma = \sqrt{2D\Delta t}$. Then, σ represents the area of influence over which two particles can come into contact and react. As demonstrated later on, the proper computation of the area of influence plays a key role in approaching realistic reactive transport solutions.

The probability of reaction P_{DB}, calculated by (28), is the probability that a pair of particles (A,B) react within a time interval Δt. Numerically, this is done by comparing a random number generated from a uniform distribution $\xi \sim U(0, 1)$ with the calculated probability. If $P_{DB} \geq \xi$, the reaction occurs and both A and B particles are removed from the system; otherwise, reaction is disregarded at that particular time step and the particle is kept. This procedure is repeated for every pair of particles (A,B) in the system. Then, the simulation continues to the next time step. At each time step, the number of remaining particles divided by N_0 represents the normalized concentration, $[A]/[A_0]$.

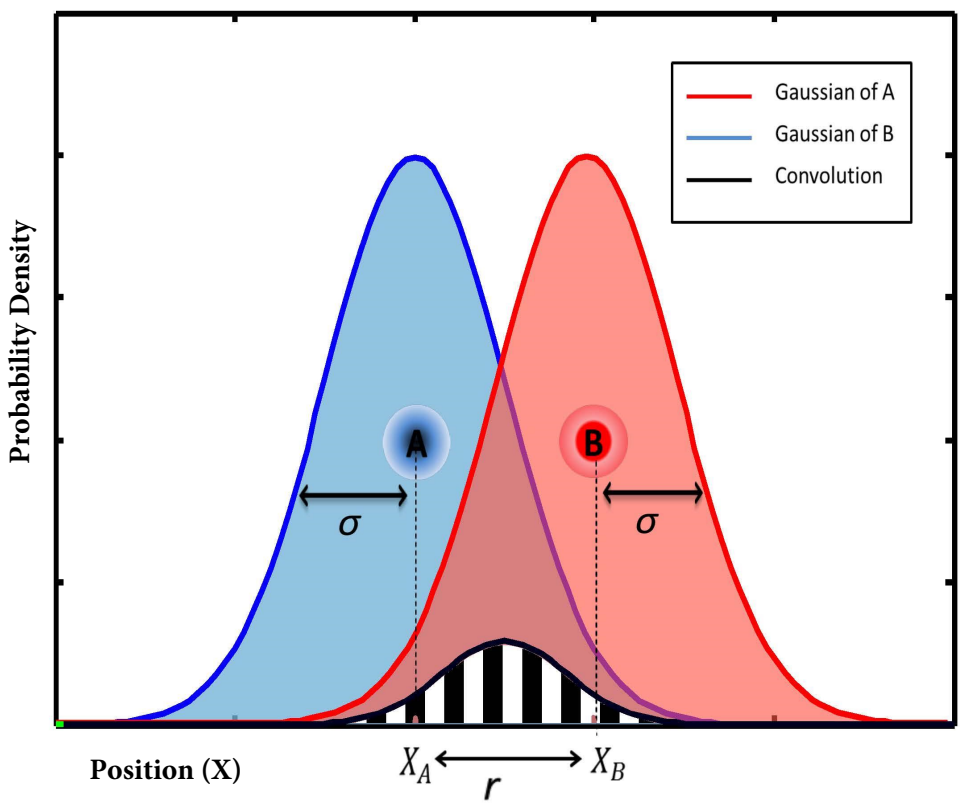

Figure 1: Convolution of two Gaussian densities with the same standard deviation σ, located at a separation distance r. The shaded area can be seen as the probability density function of the two particles A and B actually occupying the same space, so that reaction may take place according to some thermodynamic rules.

3.3 The KDE-based chemical reaction model

The DB model is characterized by a constant in time area of influence characterized by a constant diffusion, see Fig. (1). Therefore, when the number of particles is very low (occurring at late times), the probability of collocation is also very low and the segregation of particles of a given type (either A or B) start occurring (Benson and Meerschaert, 2008). Alternatively, the KDE based method provides an area of influence that increases when particles are sparsely distributed in space, see Eq. (8). This results in an enhanced probability of reaction and in an overall reaction rate approaching to the well-mixed solution, even with a small number of particles.

If the initial concentrations of the two reactants are equal, it is also logical to assign the same standard deviation to all of them, actually given by $\sigma = h^{opt}$. This dynamic bandwidth in the KDE-based model implies a different probability of reaction at each time step, preventing the formation of segregated areas of particles. The actual expression for the probability of reaction should follow rigorously the principles of the law of mass action, and also be proportional to the thermodynamic rate k_f as well as to the co-location probability density associated with the distance between particle pairs. Based on these principles, the probability of reaction for the KDE-based model is obtained as

$$P = k_f \; m_p \; \Delta t \; P_{KDE}(r), \tag{29}$$

where P_{KDE} is the convolution of the two Gaussian densities of particles A and B based on h^{opt}. This convolution is a Gaussian function with zero mean and variance equal to $2(h^{opt})^2$,

$$P_{KDE}(r) = \frac{1}{2h^{opt}\sqrt{\pi}} \; exp(\frac{-r^2}{(2h^{opt})^2}). \tag{30}$$

From Eq. (30), the probability of reaction decreases by increasing h^{opt}, preserving the unitary area under the co-location probability density. In other words, expanding the influential area of each particle by h^{opt} comes at the expense of decreasing the probability of reaction. On the other hand, as demonstrated later, this effect is compensated by the increase in the number of potentially reactive pairs, as each individual particle samples a larger area for the presence of particles. This is particularly beneficial to avoid the segregation of particles resulting in artificial poor mixing. In addition, in contrast to the DB model, P_{KDE} in Eq. (30) is not a function of the time interval Δt and the KDE model is

less sensitive to this parameter.

3.4 Simulation results

DB model

We first intend to simulate reactions with the DB model so as to later compare the performance of the KDE model with the DB model. A 1-D domain of size $\Omega = 64$ (normalized units) is considered. Simulations are performed for 10,000 time steps. The different scenarios analyzed combine different number of initial particles N_0 (always equal for species A and B), with two diffusion coefficients $D = 10^{-2}$ and $D = 10^{-5}$. The remaining parameters are set as: $[A_0] = [B_0] = 5 \times 10^{-3}$, $k_f = 50$, and $\Delta t = 0.1$. All values throughout this section are reported in normalized units.

Figure 2 shows the normalized concentration $[A]/[A_0]$ as a function of time. For comparison purposes, the analytical solution of the well-mixed system in Eq. (27) is also provided. At early times, due to the presence of a large number of particles in the system, the numerical and analytical solutions are identical. Therefore, the number of particles plays a negligible role and the actual concentration is closely approximated by the well-mixed solution, controlled simply by the thermodynamic rate coefficient k_f. However, at late times, a deviation from the analytical solution occurs, as chemical reactions among particles become limited by diffusion. In this diffusion-limited regime, islands of segregated particles (only one of the two species present) start to form, leading to a poor-mixed solution. A lower number of initial particles or a smaller diffusion constant enhances particle segregation and thereby the deviation from the well-mixed solution. These results are in a good agreement with those presented by Benson and Meerschaert (2008).

KDE model

To illustrate the potential of our proposed KDE model, a simulation of the irreversible chemical reaction is performed with a diffusion constant of $D = 10^{-2}$ and an initial number of particles of $N_0 = 4000$. The rest of the parameters are chosen equal to those used for the DB model. To effectively search for potentially reactive pairs of particles A and B, the 1-D domain is divided by elements of size $\Omega/2h^{opt}$, then we find at each element and its two neighbors, all pairs of particles A and B. Figure 3 shows the comparison between the KDE

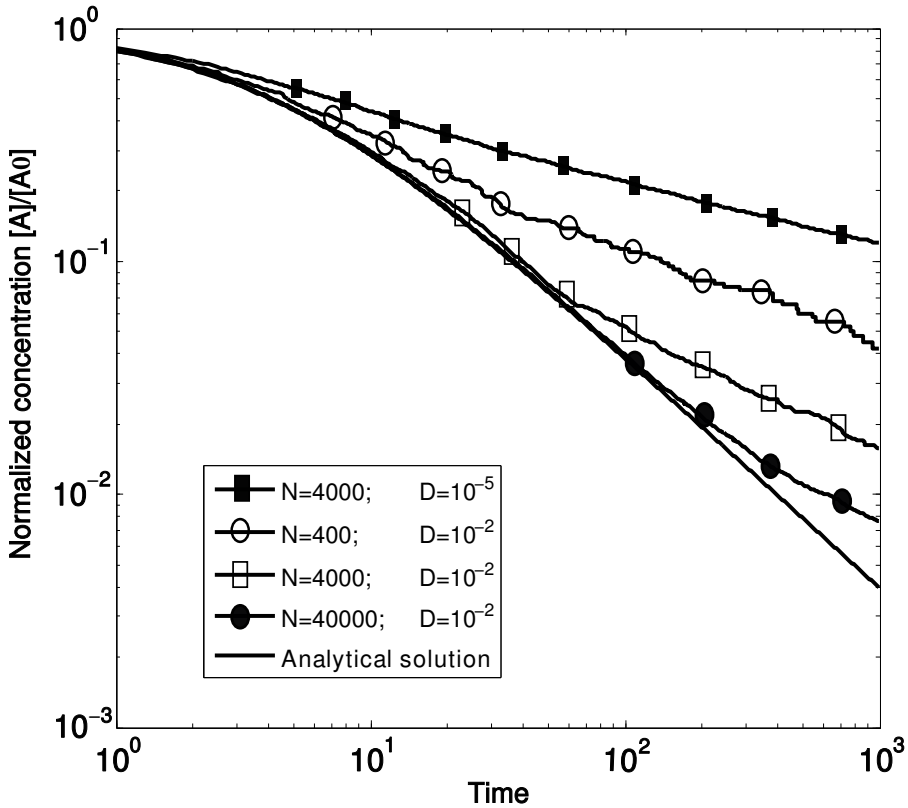

Figure 2: Normalized concentration as a function of time using the DB model. Analytical solution of the well-mixed system is also plotted for comparison purposes. The time where deviation is observed depends on the number of particles that were initially in the system. Notice that when particles are used to represent a group of molecules, the actual number used in the simulations is a modeler's choice.

and two DB models, as well as the analytical solution. Results demonstrate that the KDE model approaches the well-mixed analytical solution in a wider range of times, resulting in a considerably lower dependency of the solution on the number of particles with respect to the DB model. In fact, the simulation results for $N = 4000$ using the KDE model follows closely the results of the DB model with $N = 40{,}000$. This is an obvious enhancement of the classical chemical reaction model, as reaction rates are predicted using a noticeable lower number of particles.

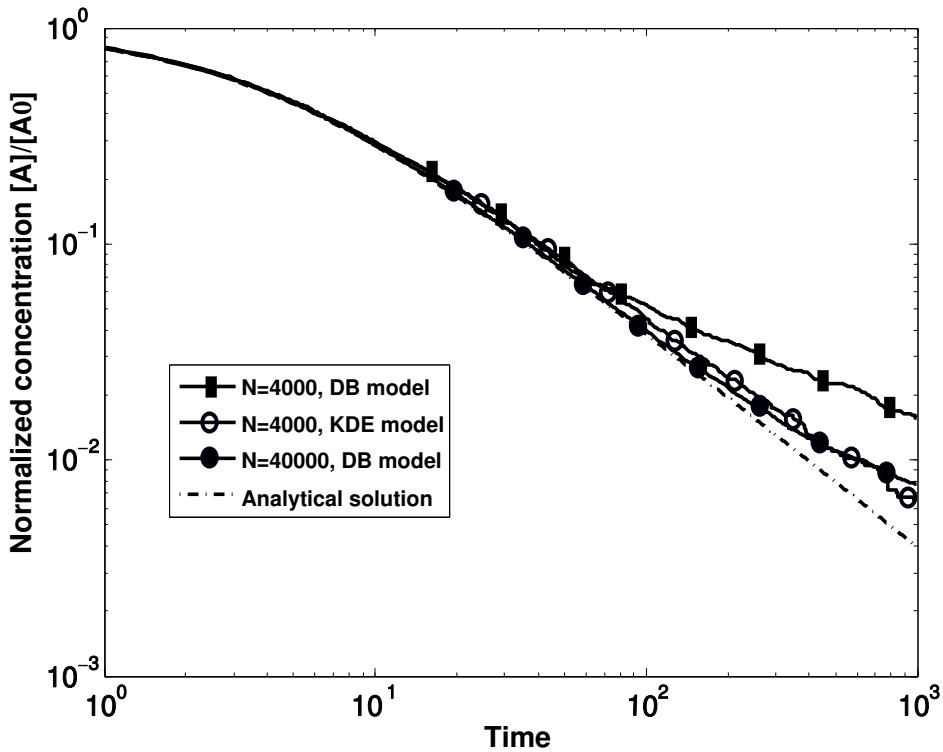

Figure 3: Normalized concentration as a function of time using the KDE model, two DB models with different number of particles, and the corresponding analytical solution.

To further illustrate the behavior of the KDE model, we perform additional simulations with a different number of particles being present at time zero. The results in Fig. 4 indicate that the decay of concentration of reactants is significantly less sensitive to the number of particles as compared to the behavior of the DB model, c.f. Fig. 2. As the solution is almost independent of the number of particles, N can be adopted by the modeler a priori solely based on the computational effort needed for the application, rather than on its potential

influence on the solution. Indirectly it also implies that it is possible to actually use a lower number of particles to achieve a given accuracy in the solution.

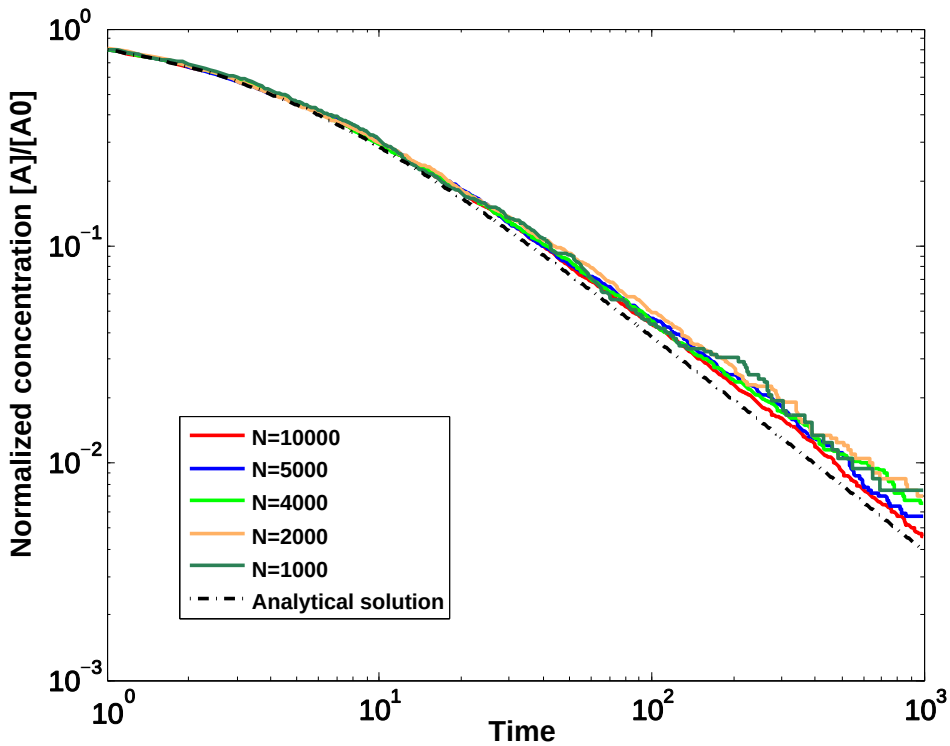

Figure 4: Normalized concentration as a function of time using the KDE model for a varying number of particles representing the initial mass. The solution is quite insensitive to the choice of number of particles being initially present in the system.

As already noted, the performance is strongly linked to the choice of the optimal bandwidth h_{opt}. This value should be continuously updated. So, there is a risk of loosing efficiency by updating h_{opt} at each time step. Here, we propose to compute h_{opt} efficiently throughout all the simulations period by extrapolating h_{opt} from the data gathered at the initial steps (early times). Figure 5 shows the true evolution of the optimal bandwidth h_{opt} as a function of the number of particles for an initial particle number of $N_0 = 4000$ (h_{opt} is updated at each time step). It is found that the optimal bandwidth increases as the number of particles decreases, closely following the slope of -1/5 (recall Eq. (8)). Therefore, h_{opt} as a number of the remaining particles in the system can be estimated by a linear extrapolation between the optimal values obtained at two different time steps (e.g., denoted by 1 and 2 in the figure). This extrapolation allows one to avoid the costly computation involved in

solving (9) at each time step. An anomalous estimation of h_{opt} at late times is also observed, corresponding to normalized concentrations of 10^{-2}, in this problem being equivalent to the presence of only 40 particles of each species in the whole domain.

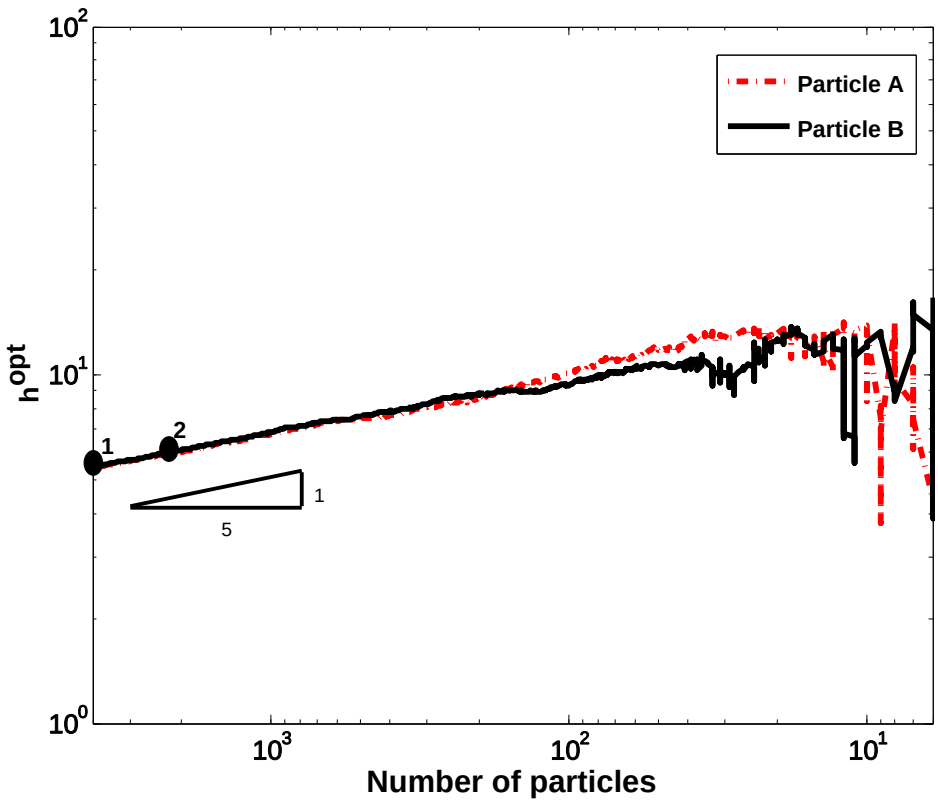

Figure 5: Optimal bandwidth as a function of the number of particles remaining in the system (not yet reacted). The points 1 and 2 represent initial steps of the simulation for the linear extrapolation of the optimal bandwidth. An slope of 1/5 for the optimal bandwidth can be considered a very good approximation up to times corresponding to very low concentrations.

3.5 Performance analysis

To systematically compare the performances of the DB and the KDE models, we define a performance factor

$$P_f = \frac{t_{max}}{t_c} + \frac{E_{max}}{E}, \tag{31}$$

where t_c is the computational time, t_{max} is the maximum of t_c among all simulations, and E is the error of the results with respect to the analytical solution, defined as

$$E = \frac{\sum_{n=1}^{s} \frac{[A]}{[A_0]}_{simulation} - \sum_{n=1}^{s} \frac{[A]}{[A_0]}_{analytical}}{\sum_{n=1}^{s} \frac{[A]}{[A_0]}_{analytical}}, \tag{32}$$

where E_{max} is the maximum error among all simulations. In Eq. (32), n stands for time step, and s is the maximum number of time steps considered in the numerical simulation. The performance factor P_f is obtained as a function of a dimensionless characteristic time τ, representing the ratio of the characteristic reaction time $T_R = (A_0 k_f)^{-1}$ to the diffusion time $T_D = L^2/D$,

$$\tau = \frac{T_R}{T_D}. \tag{33}$$

Figure 6 shows the performance factor associated with the DB and the KDE models for two different values of τ in a physically and computationally reasonable range.

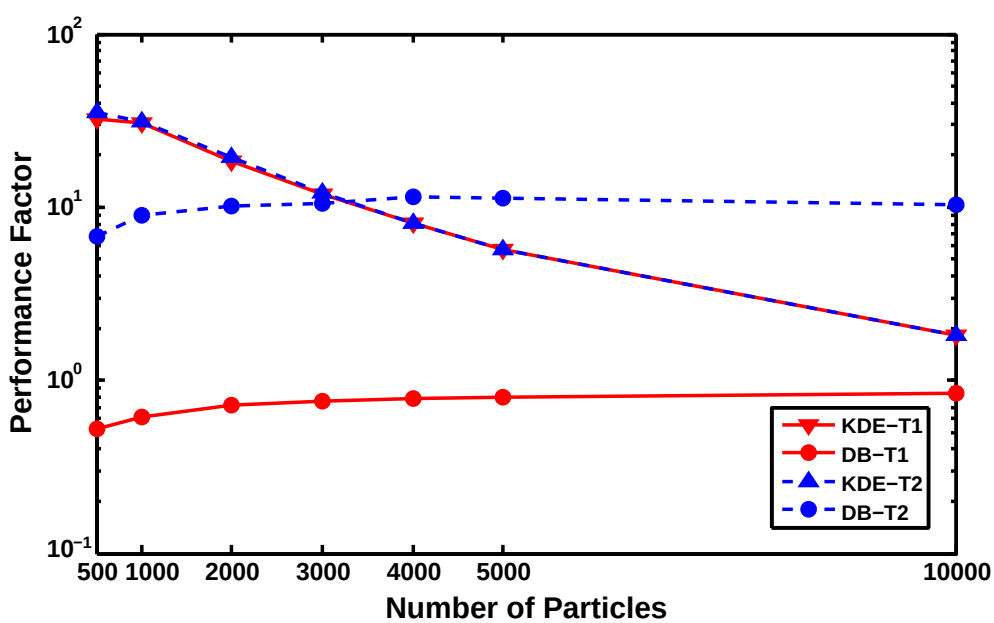

Figure 6: Performance factor as a function of the number of particles for the DB and KDE models considering two different values of the dimensionless characteristic time $\tau_1 = 9.7 \times 10^{-6}$ and $\tau_2 = 9.7 \times 10^{-9}$.

It is found that the performance factor of the KDE model is almost insensitive to the choice of τ. This implies that the kernels can adapt themselves to any parameter change, preserving the behavior of the system. Contrarily, the behavior of the DB model exhibits a strong dependence on the system parameters. It is also found that the performance factor of the KDE model is noticeably larger than that of the DB model for low number of particles and decreases by increasing this number. The main advantage of the KDE model is that the computational time increases with the number of particles while the error E does not change considerably, i.e., the first term in Eq. (31) decreases while the second term remains almost constant.

Contributions

We summarize here the most significant contributions of this work, which has been published as a research paper in (Rahbaralam et al., 2015), see Appendix A:

1. A chemical reaction model is proposed based on Kernel Density Estimators (KDEs) for the simulation of well-mixed systems. KDEs provide an optimal influential area which grows with decreasing number of particles, a feature which is beneficial to avoid incomplete mixing due to the segregation of particles.

2. Simulation results have shown a noticeable enhancement of the reaction towards the well-mixed solution when this model is applied instead of a standard PT model. Furthermore, the results of the KDE model have indicated that, in contrast to the classical DB model, the concentration decay is almost insensitive to the initial number of particles.

3. We have also conducted a performance analysis based on the computational time and error of the models. The results have shown that the performance of the KDE model does not depend on the system parameters, highlighting the rigorousness of our proposed approach. All these behaviors prove that the KDE model is a powerful tool for simulating chemical reactions of well-mixed systems.

4 Modeling of non-linear adsorption

4.1 The KDE-based adsorption model

The probability of forward reaction P_f provided in Eq. (29) was originally proposed to model a simple chemical model, i.e., the single forward bimolecular irreversible reaction. To extend this approach for modeling adsorption, P_f is considered as the probability of forward adsorption reaction in Eq. (10) with the particle C as the product of the reaction. In contrast to the bimolecular irreversible reaction, an adsorption reaction is reversible, so that a particle C can transform back to a particle A and another one B. The probability of backward desorption is given by

$$P_b = k_b \Delta t. \tag{34}$$

To numerically implement the probability of forward and backward reactions in Eqs. (29) and (34), we use the following approach. In the forward case, we first computed P_f from Eq. (29), and then we compared this value with a random number generated from a uniform distribution $\xi_f \sim U(0,1)$. Then, if $P_f \geq \xi_f$, the reaction was supposed to have occurred, and both A and B particles were removed from the system and substituted by a C particle; otherwise, the reaction was not supposed to have taken place at that particular time step and both particles were kept. This procedure was repeated for every pair of particles (A,B) in the system.

A reversed procedure was repeated for the backward reaction by comparing a random number ξ_b with the probability of backward reaction P_b obtained from Eq. (34). If $P_b \geq \xi_b$, the reaction was supposed to have occurred, the C particle was removed and substituted by an A and a B particles located at the same point C was originally considered; otherwise, no action was taken, representing that the reaction had not occurred. After the loop for all C particles were performed, the simulation continued to the next time step. We also assumed that the locations of the adsorbent particles B and the reaction product particles C were fixed (the location of the sorption sites did not change with time), so that Eq. (2) was only applied to the displacement of the adsorbate particles A. At each time step, the number of remaining particles multiplied by m_p and divided by Ω resulted in the concentrations $[A]$, $[B]$, and $[C]$. The simulation was carried out until equilibrium was clearly achieved, as

indicated by the stabilization in the ratio of concentrations $[C]/[A][B]$.

As explained later, we set up two simulation runs to assess the capacity of the model to simulate adsorption based on both the Langmuir and the Freundlich isotherms. In order to account for the former, it is just enough to set a finite number of sites $[B_0]$ and then fix the k_f and k_b values to honor the relationship set in Eq. (13). In the case of the Freundlich isotherm, it is necessary to incorporate an exponential distribution of adsorption energies, as given in Eq. (18), and to set the corresponding individual value of the equilibrium constant $\hat{K}$ at each site. The generation of the equilibrium constant $\hat{K}$ requires several considerations. As indicated in Section 2.3, the assumption of $Q_{min} \to -\infty$ in Eq. (21) is necessary for the validation of the Freundlich model in Eq. (22). However, several authors (Hill, 1949; DaRocha et al., 1997) have indicated that the integration limits over all possible adsorption energies in Eq. (17) should have a minimum cut-off to have a physical significance. To include this in our model, we consider the site-energy distribution N given by Eq. (18) as a truncated exponential distribution with cumulative distribution function given as

$$F(Q) = 1 - \exp\Big(- \frac{m}{RT}(Q - Q_{min})\Big), \quad Q \in [Q_{min}, +\infty), \tag{35}$$

where Q_{min} is the minimum energy bound. Considering Eq. (20), the cumulative distribution is obtained as a function of the equilibrium constant $\hat{K}$,

$$F(\hat{K}) = 1 - \exp(-m \ln \frac{\hat{K}}{K_{eq}} + m \ln \frac{K_{min}}{K_{eq}}), \quad \hat{K} \in [K_{min}, +\infty), \tag{36}$$

where $K_{min} = K_{eq} \exp(Q_{min}/RT)$. Notice that Eq. (36) is equivalent to a truncated power-law function, given as

$$F(\hat{K}) = 1 - \Big(\frac{\hat{K}}{K_{min}}\Big)^{-m}, \quad \hat{K} \in [K_{min}, +\infty), \tag{37}$$

with the corresponding probability density function,

$$f_{\hat{K}}(\hat{K}) = \frac{m}{K_{min}}\Big(\frac{\hat{K}}{K_{min}}\Big)^{-1-m}, \quad \hat{K} \in [K_{min}, +\infty). \tag{38}$$

Therefore, the generation of $\hat{K}$ values can be determined directly from the cumulative distribution function of $F(\hat{K})$. Given ζ to be a random value of a uniform distribution between 0 and 1, the corresponding $\hat{K}$ value is obtained as

$$\hat{K} = K_{min}(1-\zeta)^{-\frac{1}{m}}. \tag{39}$$

Rewriting Eq. (17) in terms of the probability density function of equilibrium constant $\hat{K}$ and the concentration of the adsorbed chemical compound C, we have

$$[C]_a = [B_0] \int_{K_{min}}^{+\infty} f_{\hat{K}}(\hat{K})\Theta(\hat{K})d\hat{K}. \tag{40}$$

Introducing Eq. (19) and Eq. (38) into Eq. (40) results in

$$[C]_a = m[B_0](K_{min})^m \int_{K_{min}}^{+\infty} \frac{\hat{K}^{-m}[A]}{1+\hat{K}[A]} d\hat{K}. \tag{41}$$

This integral has two limiting solutions depending on the concentration of $[A]$. When $[A]$ is small, the solution is obtained by applying a change of variable in the integration as $x = \hat{K}[A]$, so that

$$[C]_a = m[B_0](K_{min})^m[A]^m \int_{[A]K_{min}}^{+\infty} \frac{x^{-m}}{1+x} dx. \tag{42}$$

Now, we can see that the lower limit of integration approaches to zero and the solution is equivalent to

$$[C]_a = m[B_0](K_{min})^m[A]^m \int_{0}^{+\infty} \frac{x^{-m}}{1+x} dx = m[B_0](K_{min})^m[A]^m \frac{\pi}{\sin((1-m)\pi)} \tag{43}$$

Thus, when $[A] \to 0$, the concentration of the adsorbed chemical compound C follows the Freundlich isotherm written as

$$[C]_a = K[A]^m, \tag{44}$$

with

$$K = \frac{m\pi[B_0](K_{min})^m}{\sin((1-m)\pi)}. \tag{45}$$

On the contrary, when $[A]$ is large, Eq. (42) simplifies to

$$[C]_a = m[B_0](K_{min})^m[A]^m \int_{[A]K_{min}}^{+\infty} x^{-m-1}dx, \tag{46}$$

which gives

$$[C]_a = m[B_0](K_{min})^m[A]^m \frac{[A]^{-m}(K_{min})^{-m}}{m} = [B_0]. \tag{47}$$

Thus, at large concentration of $[A]$, the solution approaches the solution limit as given by the Langmuir isotherm. In short, a truncated power law distribution of equilibrium constant gives a sorption isotherm that follows the Freundlich model for small $[A]$ concentrations and changes to the Langmuir saturation limit for large $[A]$ concentrations. To understand the transition between the two limiting models, one can analyze the deviation of Eq. (41) from the Freundlich model. The relative deviation from the Freundlich model can be written as

$$\epsilon = \frac{[C]_f - [C]_a}{[C]_f} = \Big[\frac{\pi}{\sin((1-m)\pi)}\Big]^{-1}[A]^{-m} \int_0^{K_{min}} \frac{\hat{K}^{-m}[A]}{1+\hat{K}[A]}d\hat{K}. \tag{48}$$

To find an approximate solution of the relative deviation we expand the integral around $\hat{K}$=0 in an ascending series in K_{min}

$$\int_0^{K_{min}} \frac{\hat{K}^{-m}[A]}{1+\hat{K}[A]}d\hat{K} = [A]K_{min}^{-m}\Big(\frac{-K_{min}}{m-1} + \frac{[A]K_{min}^2}{m-2} - \frac{[A]^2K_{min}^3}{m-3} + ...\Big). \tag{49}$$

This is a relatively good approximation given that K_{min} is small and the integral limits are very close to each other. Truncating the series expansion at the first term results in

$$[A]_c = \Big[\frac{\epsilon\pi(1-m)}{\sin((1-m)\pi)}\Big]^{1/(1-m)} K_{min}^{-1}, \tag{50}$$

where $[A]_c$ is the concentration of $[A]$ at which the isotherm starts deviating from the Freundlich model.

The random walk model of sorption proposed here has three parameters $[B_0]$, m, and K_{min}. The parameter m represents directly the exponent of the Freundlich isotherm. The parameter K_{min} determines the maximum concentration of the chemical compound $[A]$ in the liquid phase for which sorption follows the Freundlich isotherm. The parameter $[B_0]$ is the concentration of sorption sites in the system which relates to the Freundlich coefficient

K according to Eq. (45).

4.2 Numerical simulations

The Langmuir model

The first test was design to show the performance of the proposed model to reproduce adsorption based on the Langmuir model in a batch system. The constants of forward adsorption and background desorption were set to $k_f = 0.5$ and $k_b = 0.1$, respectively. A 1-D domain of size $\Omega = 200$, a particle mass of $m_p = 1$, and initial concentration $[B_0] = 200$ are considered. Simulations are performed for 2000 time steps with a time interval of $\Delta t = 10^{-2}$ and a diffusion coefficient of $D = 10^{-2}$. All values throughout this section are reported in normalized units.

At each time step, all the adsorbate particles A are moved following Eq. (2) to account for the effect of diffusion. To effectively search for potentially reactive pairs of particles A and B, the 1-D domain is divided by elements of size $\Omega/2h^{opt}$, then we find at each element and its two neighbors, all pairs of particles A and B. The distance between each pair is first obtained, then the procedure mentioned below Eq. (34) is followed to implement the forward reaction. After repeating this procedure for every pair of particles in all elements, the backward reaction for each particle C is implemented following a similar procedure mentioned in Section 4.1.

Figure 7 shows the concentration ratio $[C]/[A][B]$ as a function of time for different initial concentration values $[A_0]$. It can be observed that all the simulations approach equilibrium at late times. Fluctuations around the equilibrium value decrease as $[A_0]$ increases. For a concentration of $[A_0] = 200$, which corresponds to an initial 40,000 particles, the actual equilibrium constant is closely approximated by the model at late times while the number of remaining adsorbate particles A in the system is very low, in the order of 1000 particles. This reasonable approximation shows the potential of our proposed model to simulate adsorption with a low number of particles. We note that the classical diffusion-based model is unable to reach this approximation due to the segregation of particles at late times (Rahbaralam et al., 2015).

To further examine the performance of the proposed model, we performed twenty simulations considering different initial concentration values $[A_0] = 40, 50, ..., 250$. For each simulation, we obtained the concentrations $[A]$ and $[C]$ from the average of their values at

the last 100 time steps (so that equilibrium was achieved). Figure 8 shows these concentrations together with the results of the analytical model in Eq. (14) for comparison purposes. It is clear that the simulation results have a good agreement with the analytical Langmuir isotherm even for a concentration of $[A] < 0.5$, where the initial number of particles is 8000 and the number of remaining adsorbate particles is below 100. By increasing the concentration $[A]$, the product concentration $[C]$ tends to saturate towards $[B_0]$ which is the maximum capacity of free sites for adsorption. This saturation level implies the mono-layer adsorption in the Langmuir isotherm.

The Freundlich model

This is a challenging model due to the need to specify different equilibrium constants to each individual sorption site. We first set up all the parameters, except k_f, identical to that of the previous section, to be consistent with the simulations for the Langmuir model. Then, according to the theoretical developments for deriving Eq. (39), the constant of forward adsorption k_f can be obtained in terms of the Freundlich constant m for each pairs of A and B particles by $k_f = k_b K_{min}(1-\zeta)^{-1/m}$, where K_{min} in the minimum equilibrium constant given by Eq. (50) and ζ is a random number generated from a standard uniform distribution. Thus, different m values were used in the simulations. Having these parameters, we followed the same procedures explained in the previous section to implement the forward and backward reactions.

To obtain a good agreement between the model and the theory, the sorption sites should follow the exponential distribution of energy in Eq. (18). However, in a range of low $[A]$ concentrations, where the number of particles is small, there is a risk of undersampling. For this reason, we performed a larger number of simulations in this range. Figure 9 shows the adsorbate concentration $[A]$ and the product concentration $[C]$ at equilibrium. It is clear that, in a range of low $[A]$ concentrations, the points in the graph follow closely a linear logarithmic slope whose value is controlled by the Freundlich constant m. By increasing the value of m, this agreement holds for a smaller range of concentrations $[A]$.

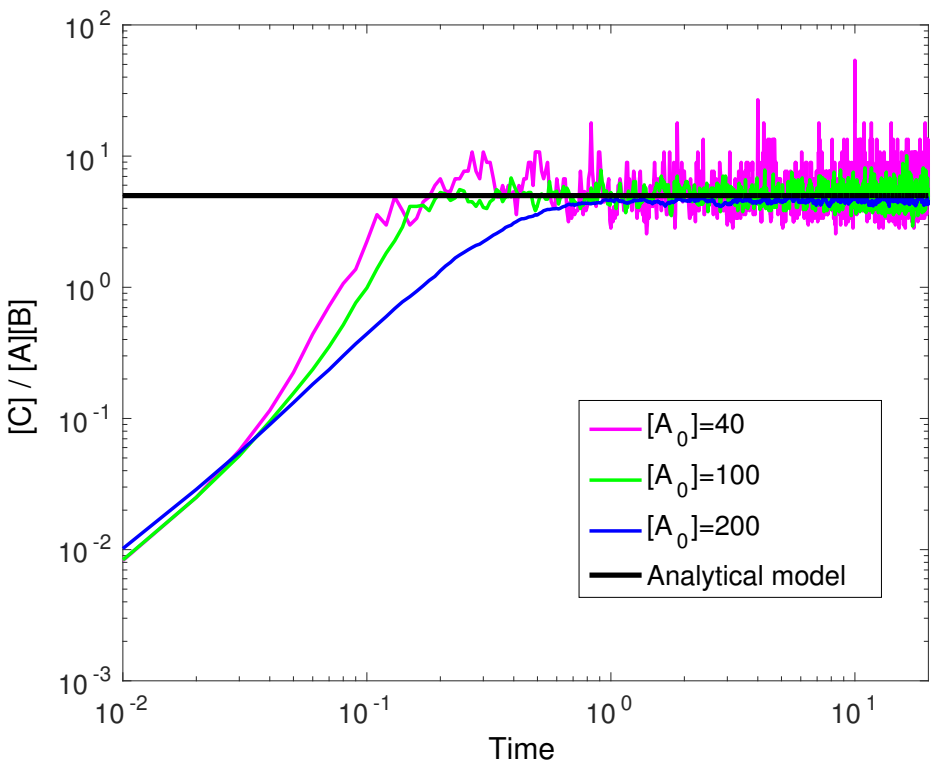

Figure 7: Concentration ratio $[C]/[A][B]$ as a function of time for different initial concentration values $[A_0]$. At equilibrium this ratio should be equal to K_{eq}, which is plotted for comparison purposes.

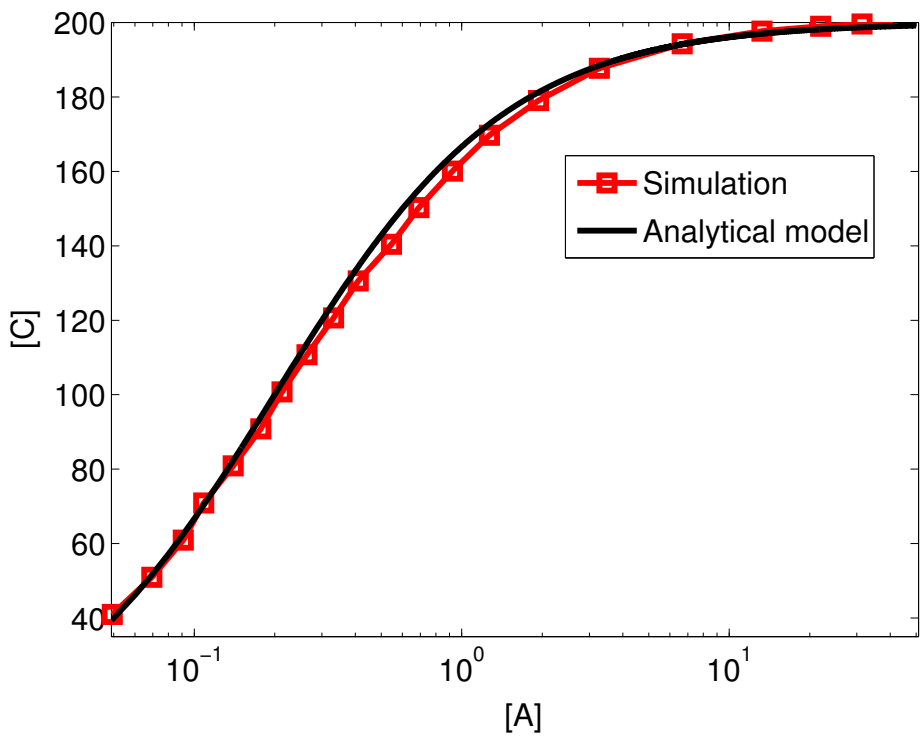

Figure 8: Concentration of the adsorbed species $[C]$ as a function of adsorbate concentration $[A]$ at equilibrium. Analytical solution of the Langmuir isotherm in Eq. (14) is also plotted for comparison purposes.

As mentioned before, a drawback of the Freundlich isotherm is that it cannot be employed for large adsorbate concentrations since this model does not taken into account the saturation limit of free adsorption sites. However, Fig. 9 indicates that the proposed model is also able to incorporate this physical limitation without the need to use a complex model that transitions to a Langmuir-type behavior. Again in Fig. 9 it is observed that as the adsorbate concentration $[A]$ increases, the number of available adsorbent sites B decreases and the product concentration $[C]$ tends to saturate to the maximum adsorbent concentration $[B_0]$. This saturation occurs at lower adsorbate concentration by increasing the value of m. Therefore, these results show that our model combines the features of both the Langmuir and Freundlich isotherms in all range of adsorbate concentrations.

One-dimensional column tracer test

To validate our proposed model, we intend to reproduce the experimental results of a one-dimensional column tracer test using lithium (Li) as reactive tracer chemical species (Fernàndez-Garcia et al., 2004). Batch experiments suggested a Freundlich behavior for the sorption of Li which agrees with experiments reported by Garabedian et al. (1988). Uniformed crushed silica sands were used to construct the column. Reactive Li tracers were injected from the inlet for an initial period of $T_0 = 60$ (min) with a concentration of $A_0 = 65.34$ (mg/L). Concentrations were measured at the outlet during 330 hours. These parameters as well as the length L and the diameter d of the column, the sand porosity ϕ, the flow rate Q, and the longitudinal dispersivity α are presented in Table 1. The flow velocity v is then obtained as $v = Q/A\phi$, where the column cross section area is given by $A = \pi d^2/4$.

The Freundlich model introduced in Section 4.1 is employed to simulate the transport of reactive species Li. We follow Eq. (3) for particle tracking where the hydrodynamic dispersion D_h is given by $D_h = D + \alpha v$. We implement this equation considering a 1-D domain of size L and a time interval of $\Delta t = 1$ min. Having these parameters, we inject an initial number of particles in each time step as $N_0 = A_0 Q \Delta t / m_p$, where m_p is the particle mass. In this simulation, we assume $m_p = 163$ ng which leads to $N_0 = 1000$. These

Table 1: Tracer test parameters

L	d	ϕ	A_0	Q	α	T_0
44.52 cm	39.5 cm	0.4	65.34 $\frac{mg}{L}$	2.5 $\frac{mL}{min}$	0.1 cm	60 min

particles are injected at the beginning of the 1-D domain for each time step until reaching the injection time T_0. An initial 55,000 adsorbent particles B and a backward desorption reaction constant $k_b = 0.3$ min^{-1} are considered. The Freundlich coefficient K was obtained by Fernàndez-Garcia et al. (2004) as $K = 1.15$ (mg/L)$^{(1-m)}$, determining the parameter $[B_0]$ according to Eq. (45). The simulation is performed for 20,000 time steps. At each time step, we count the particles which reach the end of the domain, i.e. $X_j > L$, then the normalized concentration A/A_0 is obtained as the number of the counted particles divided by N_0. Finally, the results are fitted with a two-term Gaussian function. Figure 10 shows the normalized concentration as a function of the pore volume $v.t/L$. Experimental data reported by Fernàndez-Garcia et al. (2004) is also plotted for comparison. A good match between these breakthrough curves is found for a value of $m = 0.4$, comparable to a value of $m = 0.36$ obtained from a finite difference transport model (Fernàndez-Garcia et al., 2004). Note that in this work the value of dispersion has been reported as $\alpha = 0.223$ cm while here we consider a value of $\alpha = 0.1$ cm. This difference can be attributed to the numerical dispersion induced by the finite difference method. We also note that the value of m used in the simulation should be viewed as a column-scale effective parameter and may not correspond to true Freundlich model parameter.

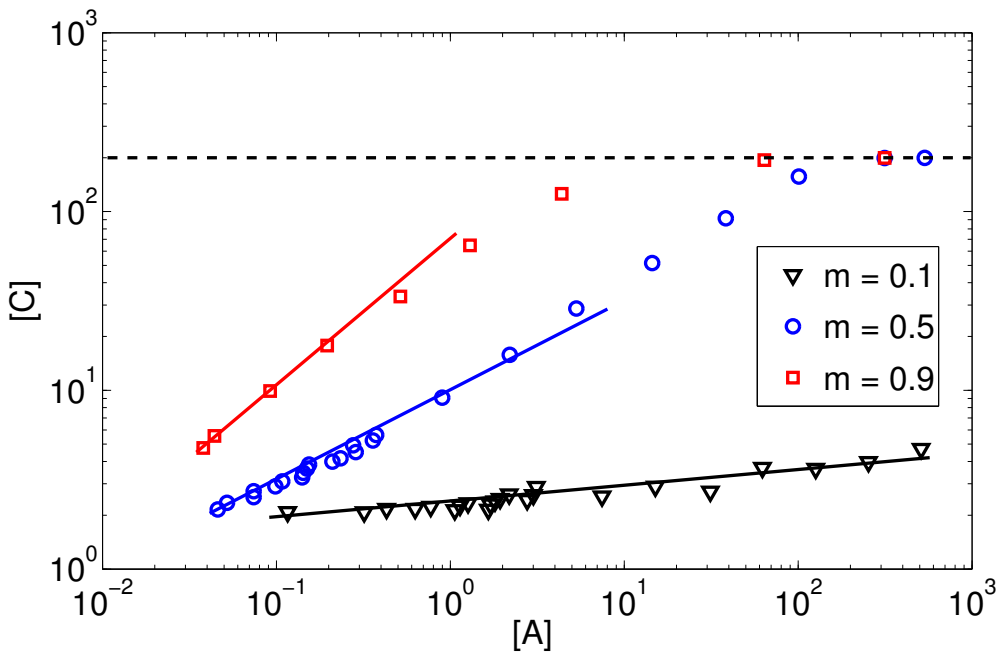

Figure 9: Concentration $[C]$ as a function of concentration $[A]$ at equilibrium. Logarithmic slope of the solid lines correspond to the Freundlich constant m values used in the simulations. The dashed line shows the saturation concentration $[B_0]$.

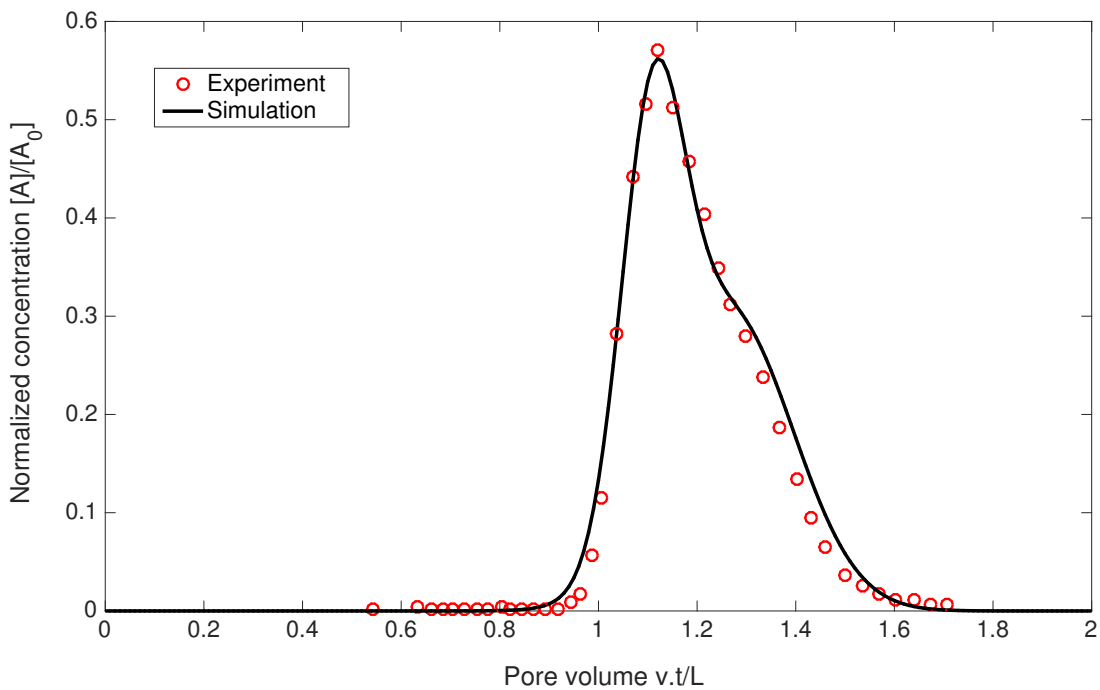

Figure 10: Normalized concentration $[A]/[A_0]$ as a function of pore volume $v.t/L$ via one-dimensional column tracer test for Lithium. Experimental results are derived from the work of Fernàndez-Garcia et al. (2004) .

Contributions

We summarize here the most significant contributions of this work:

1. We have proposed a numerical method that combines a simple Particle Tracking Methods (PTM) with some predefined rules for particle interaction that properly reproduces nonlinear adsorption. The method uses Kernel Density Estimators (KDEs), enabling it to avoid the effects of incomplete mixing due to the segregation of particles which is common in classical diffusion-based models with finite (and small) number of particles.

2. It was found that the PTM-KDE method provides a good reproduction of nonlinear adsorption following the Langmuir isotherm by simply adding a finite number of sorption sites of homogeneous sorption properties. The advantage of using KDEs is that it is possible to obtain very good results in terms of adsorbed versus adsorbate concentrations with quite a small number of particles, while other PTM methods would rely on a very large number of tracked particles to obtain good approximations. The effect of the nonlinearity resulted in a different equilibrium time depending on the initial concentration of the dissolved species (adsorbate).

3. We have also extended the approach to address nonlinear sorption modeled with a Freundlich isotherm. This involves some theoretical considerations regarding heterogeneity of the sorption properties at each specific sorption site. When such properties follow a truncated exponential statistical distribution, adsorption follows a power law in the ratio of sorbed and dissolved concentrations. This is valid for low to intermediate concentration values. The saturation of adsorbent sites has been also observed for high concentrations, pointing out the ability of our model to combine the features of the classical Langmuir and Freundlich isotherms. Our proposed approach opens up a new way to predict and control an adsorption-based process using a particle-based method with a finite (and actually quite low) number of particles.

5 Mobile-immobile model

As mentioned in Section 3, incomplete mixing in diluted systems should be modeled based on alternative mechanistic models and not on a limited number of particles. Simulation results of our proposed KDE model have already shown that the number of particles plays a negligible role on the solution and the actual concentration is closely approximated by the well-mixed solution, controlled simply by the thermodynamic rate coefficient. This potential allows us to develop a model for incomplete mixing solutions insensitive to the choice of number of particles being present in the system. While in well-mixed systems the concentrations are fully controlled by chemical processes, in many real situations spatial heterogeneities lead to a complex temporal evolution of the system, which depend on the transport and mixing mechanisms. Mixing is the ensemble of processes by which substances originally segregated into different volumes of space. This leads us to consider incomplete mixing driven by double porosity systems.

A porous medium can be regarded as consisting of two distinct domains, a mobile domain where advection-dispersion-reaction takes place and an immobile domain where transport is predominately by molecular diffusion. This physical reality of the existence of both domains has been recognised by the so-called mobile-immobile (MIM) model. This model has been used to represent physical and chemical non-equilibrium mass transfer processes controlled by diffusion that occur during solute advection and dispersion (Barenblatt et al., 1960; Coats and Smith, 1964; Deans, 1963; Gardner and Brooks, 1957). The simplest mass transfer between a mobile domain and an immobile domain is approximated as a first-order exchange dictated by a single-rate coefficient. A concise review of the many different mathematical forms of the MIM model has been presented by Haggerty and Gorelick (1995). The single-rate MIM model has been applied successfully to field problems and it has become popular among hydrologists for studying transport in saturated and unsaturated zones, and in granular as well as fractured media (Zhang and Brusseau, 1999; Feehley et al., 2000; Harvey and Gorelick, 2000; Gorelick et al., 2005). A far more comprehensive and generalized description of mass transfer between mobile and immobile domains is the multirate model, e.g. (Brusseau et al., 1989; Villermaux, 1987; Sardin et al., 1991; Valocchi, 1990) which accounts for simultaneous mass transfer processes, governed by multiple first-order equations and a set of mass transfer rate coefficients. The implementation of the MIM model into random

walk particle tracking has been presented recently by Salamon et al. (2006a). They have introduced a mechanism by which the particle is exchanged between the mobile/immobile domain in the random walk method. Here, our objective is to incorporate this mechanism in the reactive KDE model to account for the heterogeneity of porous media.

5.1 Mobile-immobile approach

By incorporating the bimolecular irreversible chemical reaction in the single-rate MIM model as one of the most commonly used models of rate-limited mass transfer (Haggerty and Gorelick, 1995), the physical model governing the chemical species A and B between mobile and immobile zones is written as:

$$\phi_m \frac{\partial [A_m]}{\partial t} + \phi_{im} \frac{\partial [A_{im}]}{\partial t} = -k_f [A_m][B_m], \tag{51}$$

$$\frac{\partial [A_{im}]}{\partial t} = \alpha([A_m] - [A_{im}]) - k_f [A_{im}][B_{im}], \tag{52}$$

$$\phi_m \frac{\partial [B_m]}{\partial t} + \phi_{im} \frac{\partial [B_{im}]}{\partial t} = -k_f [A_m][B_m], \tag{53}$$

$$\frac{\partial [B_{im}]}{\partial t} = \alpha([B_m] - [B_{im}]) - k_f [A_{im}][B_{im}], \tag{54}$$

where ϕ_m and ϕ_{im} are the mobile and immobile porosities, respectively, $[A_m]$ is the concentration of species A in the mobile zone, $[A_{im}]$ is the concentration of species A in the immobile zone, k_f is the reaction rate constant, and α is the first-order mass transfer rate coefficient. Note that a similar procedure explained in Section 3.1 is followed to derive these equations assuming a well-mixed concentration for both mobile and immobile domains. Assuming that $\phi_m = 1$ and $\phi_{im} = \beta$, β being the capacity ratio defined as $\beta = \phi_{im}/\phi_m$, Eqs. (51) and (53) convert to

$$\frac{\partial [A_m]}{\partial t} + \beta \frac{\partial [A_{im}]}{\partial t} = -k_f [A_m][B_m], \tag{55}$$

$$\frac{\partial [B_m]}{\partial t} + \beta \frac{\partial [B_{im}]}{\partial t} = -k_f [A_m][B_m]. \tag{56}$$

In the limiting case $\alpha \to \infty$, the total concentration is divided equally between the mobile and immobile zones, i.e. $[A_m] = [A_{im}]$ and $[B_m] = [B_{im}]$, and the above equations are rewritten as

$$(1+\beta)\frac{\partial[A_m]}{\partial t} = -k_f[A_m][B_m]. \tag{57}$$

$$(1+\beta)\frac{\partial[B_m]}{\partial t} = -k_f[A_m][B_m]. \tag{58}$$

Assuming that $[A_m] = [B_m]$, the analytical solution of Eqs. (57) and (58) is obtained as

$$[A_m] = \frac{[A_{m_0}]}{1+[A_{m_0}]k_f t'}, \tag{59}$$

where $[A_{m_0}]$ is the initial concentration in the mobile zone and $t' = t/(1+\beta)$, t being time. The total concentration $[A]$ over total volume when $\alpha \to \infty$ is obtained as

$$[A] = (1+\beta)[A_m] = \frac{(1+\beta)[A_{m_0}]}{1+[A_{m_0}]k_f t'} = \frac{[A_0]}{1+[A_0]k_f \hat{t}}, \tag{60}$$

where $[A_0] = (1+\beta)[A_{m_0}]$ and $\hat{t} = t'/(1+\beta) = t/(1+\beta)^2$. Therefore, in the limiting case $\alpha \to \infty$, the total concentration $[A]$ decays with a time delay factor $(1+\beta)^2$.

Following the recent work of Salamon et al. (2006a), the change in the state of a particle from the mobile state to the immobile state is determined using transition probabilities. The transition probability, $P_{ij}(\Delta t)$, that a particle presently in state i (mobile) will be in state j (immobile) at a time $t + \Delta t$ is given by

$$\boldsymbol{P}(\Delta t) = \begin{pmatrix} \frac{1+\beta e^{-(1+\beta)\alpha\Delta t}}{1+\beta} & \frac{1-e^{-(1+\beta)\alpha\Delta t}}{1+\beta} \\ \frac{\beta-\beta e^{-(1+\beta)\alpha\Delta t}}{1+\beta} & \frac{\beta+e^{-(1+\beta)\alpha\Delta t}}{1+\beta} \end{pmatrix} \tag{61}$$

If a particle is in the mobile domain, then it is susceptible to dispersion and reaction, otherwise the particle is not allowed to move and react with other particles (immobile). Having calculated the phase transition probabilities, numerical implementation into particle tracking is done following the same procedure explained in Section 3. For each time step a uniform [0,1] random number is drawn for each particle and is compared to the corresponding probability. The state of a particle being in the mobile phase is adjusted accordingly.

5.2 Simulation results

We perform the first set of simulations considering a fixed value of $\beta = 1$ and different values of α. A 1-D domain of size $\Omega = 64$ (normalized units), diffusion coefficient $D = 10^{-5}$, reaction coefficient $k_f = 50$, $[A_0] = [B_0] = [A_{m0}] = [B_{m0}] = 5 \times 10^{-3}$, and $\Delta t = 0.1$ is considered. Simulations are performed for 10,000 time steps. All values are reported in normalized units. Having considered the transition probability in Eq. (61), we follow the same procedure introduced in Section 3 for the KDE model to compute the reaction probability and the movement of mobile particles. Figure 11 shows the normalized concentration $[A]/[A_0]$ as a function of time. The analytical solution of the well-mixed system (complete mixing) in Eq. (27) is also presented for comparison purposes. It is clear that by choosing an infinitesimal value of $\alpha = 10^{-5}$, the result approaches the solution of the well-mixed system. The reason is that the transition probability density $P_{m,im}$ in Eq. (61) tends to zero in the limit of $\alpha \to 0$, preventing the transition of particles from the mobile to the immobile state. In the absence of immobile particles, the system recovers the complete mixing state, as presented in Section 3. On the other hand, for a large value of $\alpha = 10^3$, the total concentration is divided equally between the mobile and immobile zones, i.e. $[A_m] = [A_{im}]$, and the result tends to the analytical solution in Eq. (60) with a time delay factor $(1 + \beta)^2$. For intermediate values of α, the results show a transition between the two limiting cases.

To further investigate the behavior of the model in the limiting case $\alpha \to \infty$, we perform simulations considering different values of β and a fixed value of $\alpha = 10^3$. Figure 12 shows the normalized concentration $[A]/[A_0]$ as a function of time. For each chosen value of β, the analytical solution in Eq. (60) is also plotted for comparison purposes. Simulation results show a good agreement with the analytical solutions, indicating that by increasing the capacity ratio β, the system tends to the incomplete mixing solution. In fact, in the limit of $\beta \to \infty$, all the particles are trapped in the immobile domain with a volume of $V_{im} \to \infty$ and the incomplete mixing solution is recovered, i.e. total concentration $[A]$ remains constant as a function of time.

In the absence of an analytical solution for the transition curves between the limiting cases $\alpha \to 0$ and $\alpha \to \infty$, we perform a curve fitting of the results for intermediate values $\alpha = 10^{-1}$, $\alpha = 10^{-2}$, and $\alpha = 10^{-3}$ in Fig. 11 using the following equation,

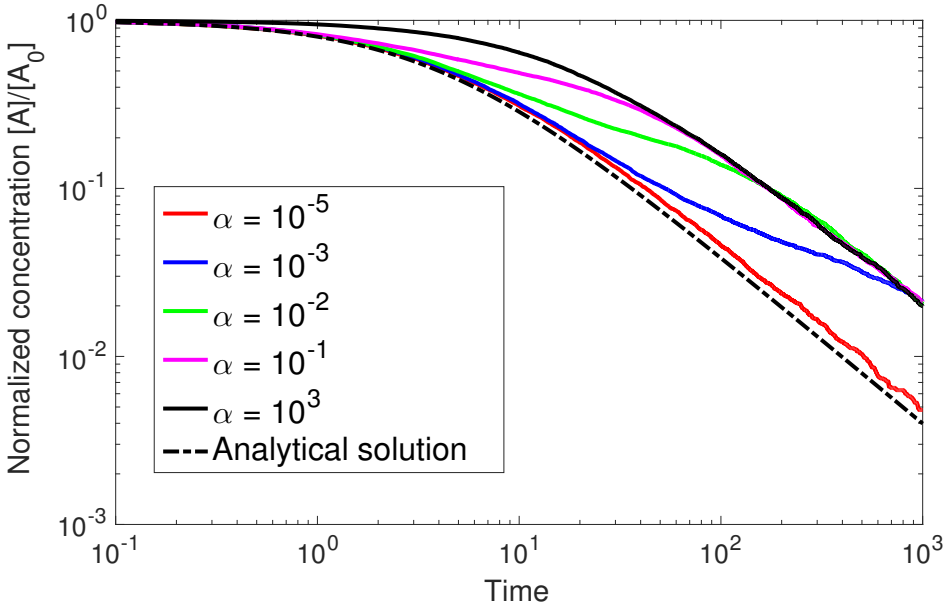

Figure 11: Normalized concentration $[A]/[A_0]$ as a function of time considering different values of α and a value of $\beta = 1$. Analytical solution of the well-mixed system in the absence of the immobile domain is plotted for comparison purposes.

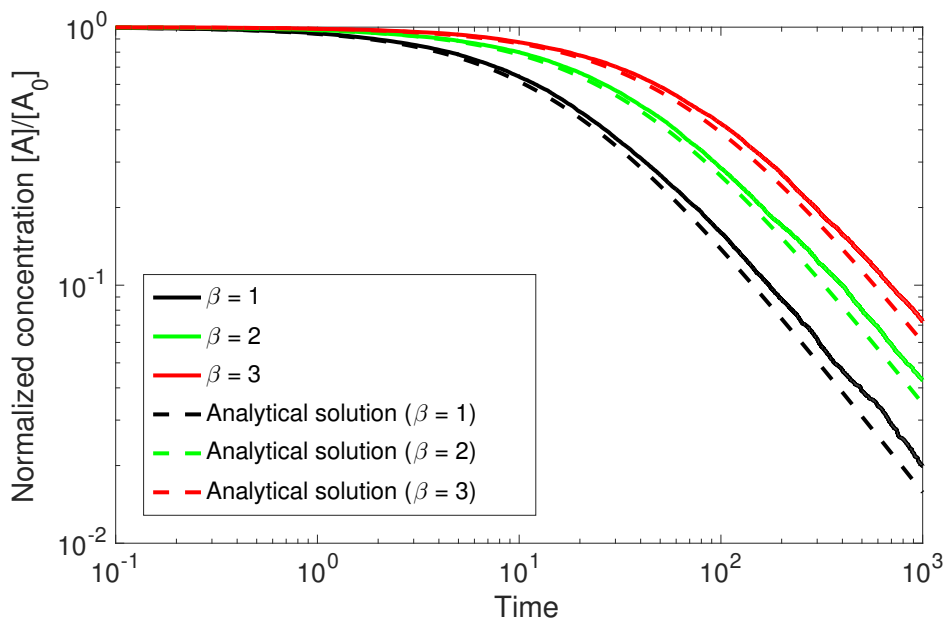

Figure 12: Normalized concentration $[A]/[A_0]$ as a function of time considering different values of β and a value of $\alpha = 10^3$. Analytical solutions are plotted for comparison purposes.

$$[A] = \frac{[A_0]}{1 + [A_0]\hat{k}_f(t)t}, \tag{62}$$

where the modified reaction coefficient $\hat{k}_f(t)$ is defined as a function of time following a transition probability,

$$\hat{k}_f(t) = k_f\Big(\frac{1 + \beta' e^{-(1+\beta')\alpha' t}}{1 + \beta'}\Big), \tag{63}$$

where α' and β' are the fitting parameters. Considering Eq. (63) and having known that $\hat{k}_f(t) = k_f$ for $t \to 0$ and $\hat{k}_f(t) = k_f/(1+\beta)^2$ for $t \to \infty$, then the parameter β' is obtained as a function of β as $(1+\beta') = (1+\beta)^2$. Therefore, α' remains as the only fitting parameter. Figure 13 shows the simulation results together with the fitted curves. The obtained values of the fitting parameter α' are comparable with the chosen values of the mass transfer rate coefficient α, indicating that Eq. (63) provides a simple estimate of the transition between the limiting cases $\alpha \to 0$ and $\alpha \to \infty$.

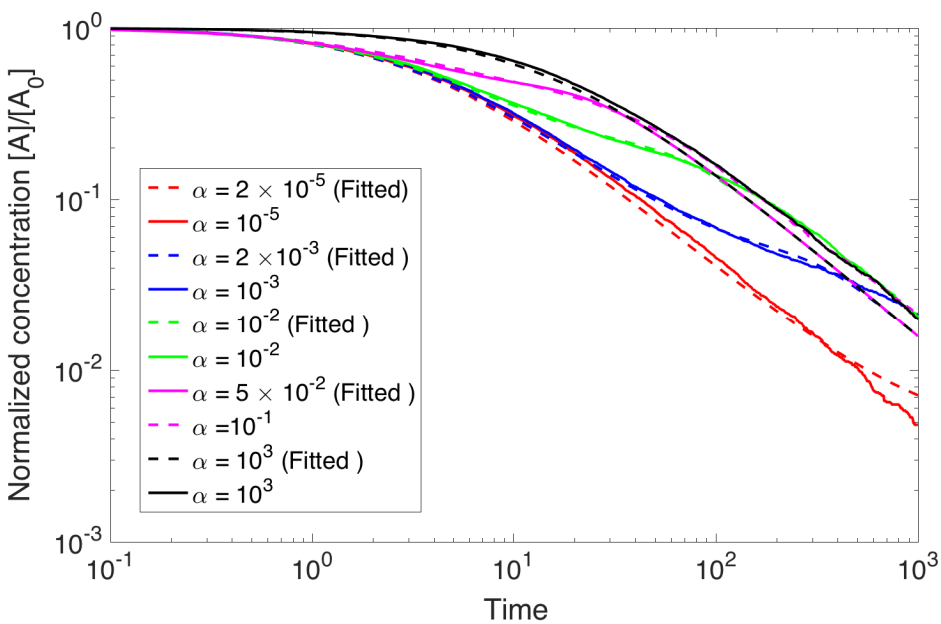

Figure 13: Normalized concentration $[A]/[A_0]$ as a function of time considering different values of α and a value of $\beta = 1$. A curve is fitted for each set of results according to Eq. (63) with a fitting parameter α' and $\beta' = 3$.

These results show the potential of the extended KDE-based approach to control mixing

(complete to incomplete) by the parameters α and β originated from a mechanistic model rather than by numerical parameters such as the number of particles, c.f. Figs. 2 and 13.

Contributions

We summarize here the most significant contributions of this work:

1. The KDE-based approach introduced in Section 3 is extended to the mobile-immobile (MIM) model for the simulation of reactive transport in heterogenous porous media. The extended MIM model separates the particles to mobile and immobile states and the change between these two states is determined using transition probabilities.

2. Simulation results have indicated that the extended MIM model is able to control mixing using mechanistic parameters such as the mass transfer rate coefficient and the mobile and immobile porosities rather than numerical parameters such as the number of particles.

6 Conclusions

This section summarizes the main contributions and research ideas of the thesis outlined as follows:

- We propose a chemical reaction model based on Kernel Density Estimators (KDEs) for the simulation of well-mixed systems. KDEs provide an optimal influential area which grows with decreasing number of particles, a feature which is beneficial to avoid incomplete mixing due to the segregation of particles.

- Simulation results have shown a noticeable enhancement of the reaction towards the well-mixed solution when this model is applied instead of a standard PT model. Furthermore, the results of the KDE model have indicated that, in contrast to the classical DB model, the concentration decay is almost insensitive to the initial number of particles.

- We have conducted a performance analysis based on the computational time and error of the models. The results have shown that the performance of the KDE model does not depend on the system parameters, highlighting the rigorousness of our proposed approach. All these behaviours prove that the KDE model is a powerful tool for simulating chemical reactions of well-mixed systems.

- We have extended the KDE model to account for nonlinear adsorption following the Langmuir isotherm by simply adding a finite number of sorption sites of homogeneous sorption properties. The advantage of using KDEs is that it is possible to obtain very good results in terms of adsorbed versus adsorbate concentrations with quite a small number of particles, while other PTM methods would rely on a very large number of tracked particles to obtain good approximations. The effect of the nonlinearity resulted in a different equilibrium time depending on the initial concentration of the dissolved species (adsorbate).

- We have also addressed nonlinear sorption modeled with a Freundlich isotherm. This involves some theoretical considerations regarding heterogeneity of the sorption properties at each specific sorption site. When such properties follow a truncated exponential statistical distribution, adsorption follows a power law in the ratio of sorbed

and dissolved concentrations. This is valid for low to intermediate concentration values. The saturation of adsorbent sites has been also observed for high concentrations, pointing out the ability of our model to combine the features of the classical Langmuir and Freundlich isotherms. Our proposed approach opens up a new way to predict and control an adsorption-based process using a particle-based method with a finite (and actually quite low) number of particles.

- The KDE-based approach is also extended for the simulation of reactive transport in heterogenous porous media. The extended model separates the particles to mobile and immobile states and the change between these two states is determined using transition probabilities. Simulation results have indicated that the extended model is able to control mixing using mechanistic parameters such as the mass transfer rate coefficient and the mobile and immobile porosities rather than numerical parameters such as the number of particles.

The work carried out in this thesis also leaves some open research lines for the future. We suggest the following lines:

- *Particle injection:* The results of this thesis indicate a good match with the analytical results. However, we can still observe a small deviation from the analytical results. This is mainly attributed to a poor estimation of KDEs due to a low number of particles at late times. We can tackle this problem by injecting a number of particles at late times for a better estimation of KDEs. The main challenge is to find a proper particle injection method which avoids artificial numerical effects on the results.

- *Multirate modeling of complicated reactions:* The proposed models can simulate simple reactions with two or three different species dictated by a single-rate coefficient. However, for real problems involving different species and various immobile domains, more sophisticated reactions dictated by multi-rate coefficients are required. For this purpose, our proposed KDE model can be extended following different chemical reaction algorithms proposed by Gillespie et al. (2013) and the multi-rate mass transfer model proposed by Haggerty and Gorelick (1995). We expect that implementing these extensions will boost up the potential of our model for future applications.

- *Extending the model to two and three dimensions:* To produce more realistic simulations results and to capture complex chemical reactions, it is necessary to extend the 1-D model to two and three-dimensions. The main challenge towards this goal is to implement computationally efficient routines for the particle tracking method and estimation of KDEs. One of the future tasks is to implement a parallel computing technique for performing the simulations on a computer cluster. There are several challenges in this way: 1- applying scheduling tasks at the right granularity onto the processors of a parallel machine, 2- scalability support in hardware with respect to the bandwidth and interconnect between processing elements, and (3) scalability support in software such as libraries and algorithms. In addition, a domain decomposition method would be required to speed up the calculations .

Bibliography

Barenblatt, G. I., I. P. Zheltov, and I. N. Kochina (1960). Basic concepts in the theory of seepage of homogeneous liquids in fissured rocks [strata]. *J. Appl. Math. Mech. 24*(5), 1286 – 1303.

Benson, D. A. and M. M. Meerschaert (2008). Simulation of chemical reaction via particle tracking: Diffusion-limited versus thermodynamic rate-limited regimes. *Water Resour. Res. 44*, W12201.

Benson, D. A. and M. M. Meerschaert (2009). A simple and efficient random walk solution of multi-rate mobile/immobile mass transport equations. *Adv. Water Resour. 32*, 532–539.

Bolster, D., P. de Anna, D. A. Benson, and A. M. Tartakovsky (2012). Incomplete mixing and reactions with fractional dispersion. *Adv. Water Resour. 37*, 86–93.

Boso, F., A. Bellin, and M. Dumbser (2013). Numerical simulations of solute transport in highly heterogeneous formations: A comparison of alternative numerical schemes. *Adv. Water Resour. 52*, 178–189.

Brusseau, M. L., R. E. Jessup, and P. S. C. Rao (1989). Modeling the transport of solutes influenced by multiprocess nonequilibrium. *Water Resour. Res. 25*(9), 1971–1988.

Castro-Alcala, E., D. Fernàndez-Garcia, J. Carrera, and D. Bolster (2012). Visualization of mixing processes in a heterogeneous sand box aquifer. *Env. Sci. Tech. 46*, 3228–3235.

Coats, K. H. and B. D. Smith (1964). Dead-end pore volume and dispersion in porous media. *Soc. Petrol. Eng. J. 4*(1).

DaRocha, M. S., K. Iha, A. C. Faleiros, E. J. Corat, and M. E. V. Suarez-Iha (1997). Freundlich's isotherm extended by statistical mechanics. *J. Coll. Inter. Sci. 185*(2), 493 – 496.

Davis, R. T. (1946). The activated adsorption of nitrogen on a finely divided tungsten powder. *J. Am. Chem. Soc. 68*, 1395.

Deans, H. A. (1963). A mathematical model for dispersion in the direction of flow in porous media. *Trans. Soc. Petrol. Eng. J. 3*(1).

Ding, D., D. A. Benson, A. Paster, and D. Bolster (2013). Modeling bimolecular reactions and transport in porous media via particle tracking. *Adv. Water Resour. 53*, 56–65.

Feehley, C. E., C. Zheng, and F. J. Molz (2000). A dual-domain mass transfer approach for modeling solute transport in heterogeneous aquifers: Application to the macrodispersion experiment (made) site. *Water Resour. Res. 36*(9), 2501–2515.

Fernàndez-Garcia, D., T. H. Illangasekare, and H. Rajaram (2004). Conservative and sorptive forced-gradient and uniform flow tracer tests in a three-dimensional laboratory test aquifer. *Water Resour. Res. 40*, W10103–17.

Fernàndez-Garcia, D. and X. Sanchez-Vila (2011). Optimal reconstruction of concentrations, gradients and reaction rates from particle distributions. *J. Contam. Hydrol. 120-121*, 99–114.

Frankenburg, W. G. (1944). The adsorption of hydrogen on tungsten. *J. Am. Chem. Soc. 66*, 1827–1838.

Freundlich, U. (1906). *Über die Adsorption in Lösungen*. W. Engelmann.

Garabedian, S. P., L. W. Gelhar, and M. A. Celia (1988). Large-scale dispersive transport in aquifers: Field experiments and reactive transport theory. *Rep. 315*, W10103–17.

Gardner, W. R. and R. H. Brooks (1957). A descriptive theory of leaching. *Soil Sci. 83*(4).

Gillespie, D. T. (1976). A general method for numerically simulating the stochastic time evolution of coupled chemical reactions. *J. Comput. Phys. 22*, 403–434.

Gillespie, D. T. (1977). Exact stochastic simulation of coupled chemical reactions. *J. Phys. Chem. 81*, 2340–2361.

Gillespie, D. T. (2000). The chemical langevin equation. *J. Chem. Phys. 113*, 297–306.

Gillespie, D. T., A. Hellander, and L. R. Petzold (2013). Perspective: Stochastic algorithms for chemical kinetics. *J. Chem. Phys. 138*(17), 170901.

Gogoi, S. B. (2011). Adsorption-desorption of surfactant for enhanced oil recovery. *Transp. Porous Med. 90*, 589–604.

Gorelick, S. M., G. Liu, and C. Zheng (2005). Quantifying mass transfer in permeable media containing conductive dendritic networks. *Geophys. Resear. Lett. 32*(18).

Gramling, C. M., C. F. Harvey, and L. C. Meigs (2002). Reactive transport in porous media: a comparison of model prediction with laboratory visualization. *Environ. Sci. Technol. 36*, 2508–2514.

Haggerty, R. and S. M. Gorelick (1995). Multiple-rate mass transfer for modeling diffusion and surface reactions in media with pore-scale heterogeneity. *Water Resour. Res. 31*, 2383–2400.

Harvey, C. and S. M. Gorelick (2000). Rate-limited mass transfer or macrodispersion: Which dominates plume evolution at the macrodispersion experiment (made) site? *Water Resour. Res. 36*(3), 637–650.

Henri, C. V. and D. Fernàndez-Garcia (2014). Toward efficiency in heterogeneous multi-species reactive transport modeling: A particle-tracking solution for first-order network reactions. *Water Resour. Res. 50*, 7206–7230.

Herrera, P. A., A. J. Valocchi, and R. D. Beckie (2010). A multidimensional streamline-based method to simulate reactive solute transport in heterogeneous porous media. *Adv. Water. Resour. 33*(7), 711 – 727.

Hill, T. L. (1949). Statistical mechanics of adsorption. vi. localized unimolecular adsorption on a heterogeneous surface. *J. Chem. Phys. 17*(9), 762–771.

Jones, M. C., J. S. Marron, and S. J. Sheather (1996). A brief survey of bandwidth selection for density estimation. *J. Am. Stat. Assoc. 91*, 401–407.

Kang, K. and S. Redner (1985). Fluctuation-dominated kinetics in diffusion-controlled reactions. *Phys. Rev. A. 32*, 435–447.

Langmuir, I. (1918). The adsorption of gases on plane surfaces of glass, mica, and platinum. *J. Am. Chem. Soc. 40*, 1361.

Li, D. D., A. D. Jacobson, and D. J. McInerneya (2014). A reactive-transport model for examining tectonic and climatic controls on chemical weathering and atmospheric CO2 consumption in granitic regolith. *Chem. Geol. 365*, 30–42.

Moroni, M., N. Kleinfelter, and J. H. Cushman (2007). Analysis of dispersion in porous media via matched-index particle tracking velocimetry experiments. *Adv. Water. Resour. 30*, 1–15.

Ovchinnikov, A. A. and Y. B. Zeldovich (1978). Role of density fluctuations in bimolecular reaction kinetics. *Chem. Phys. 28*, 215–218.

Park, B. U. and J. S. Marron (1990). Comparison of data-driven bandwidth selectors. *J. Am. Stat. Assoc. 85*, 66–72.

Paster, A., D. Bolster, and D. A. Benson (2013). Particle tracking and the diffusion-reaction equation. *Water Resour. Res. 49*, 1–6.

Paster, A., D. Bolster, and D. A. Benson (2014). Connecting the dots: Semi-analytical and random walk numerical solutions of the diffusion-reaction equation with stochastic initial conditions. *J. Comput. Phys. 263*, 91–112.

Pedretti, D. and D. Fernàndez-Garcia (2013). An automatic locally-adaptive method to estimate heavily-tailed breakthrough curves from particle distributions. *Adv. Water Resour. 59*, 52–65.

Pollock, D. (1988). Semianalytical computation of path lines for finite-difference models. *Ground Water 26*, 743–750.

Rahbaralam, M., D. Fernandez-Garcia, and X. Sanchez-Vila (2015). Do we really need a large number of particles to simulate bimolecular reactive transport with random walk methods? a kernel density estimation approach. *J. Comput. Phys. 303*, 95 –104.

Raje, D. S. and V. Kapoor (2000). Experimental study of bimolecular reaction kinetics in porous media. *Environ. Sci. Technol. 34*, 1234–1239.

Riva, M., A. Guadagnini, D. Fernàndez-Garcia, X. Sanchez-Vila, and T. Ptak (2008). Relative importance of geostatistical and transport models in describing heavily tailed breakthrough curves at the lauswiesen site. *J. Contam. Hydrol. 101*(1), 1 – 13.

Rosenblatt, M. (1956). Remarks on some nonparametric estimates of a density function. *Annals Math. Stat. 27*, 832–837.

Salamon, P., D. Fernàndez-Garcia, and J. J. Gomez-Hernandez (2006a). Modeling mass transfer processes using random walk particle tracking. *Water Resour. Res. 42*, 1234–1239.

Salamon, P., D. Fernàndez-Garcia, and J. J. Gomez-Hernandez (2006b). A review and numerical assessment of the random walk particle tracking method. *J. Contam. Hydrol. 87*, 277–305.

Sanchez-Vila, X., D. Fernàndez-Garcia, and A. Guadagnini (2010). Interpretation of column experiments of transport of solutes undergoing an irreversible bimolecular reaction using a continuum approximation. *Water Resour. Res. 46*, 1–7.

Sardin, M., D. Schweich, F. J. Leij, and M. T. van Genuchten (1991). Modeling the nonequilibrium transport of linearly interacting solutes in porous media: A review. *Water Resour. Res. 27*(9), 2287–2307.

Saurabh, P. and S. Chakraborty (2009). Mathematical modeling of reactive transport of anti-tumor drugs through electro-active membranes. *Asia-Pacific J. Chem. Eng. 4*, 345–355.

Sheindorf, C., M. Rebhum, and M. A. Sheintuch (1981). Freundlich-type multicomponent isotherm. *J. Colloid Inter. Sci. 79*, 136–142.

Siirila-Woodburn, E. R., D. Fernàndez-Garcia, and X. Sanchez-Vila (2015). Improving the accuracy of risk prediction from particle-based breakthrough curves reconstructed with kernel density estimators. *Water Resour. Res. 51*, 4574–4591.

Sips, R. (1948). On the structure of a catalyst surface. *J. Chem. Phys. 16*, 490–495.

Tartakovsky, A. M. and P. Meakin (2005). A smoothed particle hydrodynamics model for miscible flow in three-dimensional fractures and the two-dimensional rayleigh-taylor instability. *J. Comput. Phys. 207*, 610–624.

Thomas, W. J. (1957). Chemisorption of ethane at iron and nickel oxide. *Trans. Faraday Soc. 53*(1124-1131).

Tompson, A. F. B. and D. E. Dougherty (1992). Particle-grid methods for reacting flows in porous media with application to fisher's equation. *Appl. Math. Model. 16*, 374–383.

Urano, K., Y. Koichi, and Y. Nakazawa (1981). Equilibria for adsorption of organic compounds on activated carbons in aqueous solutions i. modified freundlich isotherm equation and adsorption potentials of organic compounds. *J. Colloid Interface Sci. 81*, 477–485.

Valocchi, A. J. (1990). Use of temporal moment analysis to study reactive solute transport in aggregated porous media. *Geoderma 46*(1), 233 – 247.

Villermaux, J. (1987). Chemical engineering approach to dynamic modelling of linear chromatography. *J. Chromatography A 406*, 11 – 26.

Willmann, M., J. Carrera, X. Sanchez-Vila, O. Silva, and M. Dentz (2010). Coupling of mass transfer and reactive transport for nonlinear reactions in heterogeneous media. *Water Resour. Res. 46*, W07512.

Xu, T., L. Zheng, and H. Tian (2011). Reactive transport modeling for CO2 geological sequestration. *J. Petrol. Sci. Eng. 78*, 765–777.

Zhang, Z. and M. L. Brusseau (1999). Nonideal transport of reactive solutes in heterogeneous porous media: 5. simulating regional-scale behavior of a trichloroethene plume during pump-and-treat remediation. *Water Resour. Res. 35*(10), 2921–2935.

Do we really need a large number of particles to simulate bimolecular reactive transport with random walk methods? A kernel density estimation approach

M. Rahbaralam, D. Fernández and X. Sánchez

Journal of Computational Physics

303, 94-105, 2015